Available online at www.sciencedirect.com
SCIENCE DIRECT
Agricultural and Forest Meteorology 137 (2006) 194–219
AGRICULTURAL AND FOREST METEOROLOGY
www.elsevier.com/locate/agrformet

Simulation of diurnal variations of CO_2, water and heat fluxes over winter wheat with a model coupled photosynthesis and transpiration

Jing Wang [a,b], Qiang Yu [a,*], Jun Li [a], Long-Hui Li [a], Xiang-Ge Li [c], Gui-Rui Yu [a], Xiao-Min Sun [a]

[a] *Institute of Geographical Sciences and Natural Resources Research, Chinese Academy of Sciences, A11 Datun Road, Beijing 100101, PR China*
[b] *Graduate School of the Chinese Academy of Sciences, Beijing 100039, PR China*
[c] *Department of Applied Meteorology, Nanjing University Information Science and Technology, Nanjing 210044, PR China*

Received 29 December 2003; received in revised form 24 May 2005; accepted 28 February 2006

Abstract

A model was developed that couples canopy photosynthesis and transpiration of winter wheat. The model combined a two-layer evapotranspiration model with a coupled photosynthesis–stomatal conductance model to study the diurnal variations of CO_2, water and heat fluxes of winter wheat. Field experiments were conducted in Yucheng Comprehensive Experimental Station in the North China Plain to evaluate the model. Half-hourly data of weather variables and CO_2, water and heat fluxes were measured by the eddy covariance method in 2002–2003. An analysis of measured flux data showed that there was an evident midday depression of photosynthesis, caused by stomatal closure due to high vapor water deficit and canopy temperature though the soil was well irrigated. There was a close agreement between simulated and measured net radiation, CO_2 flux, sensible and latent heat fluxes, which proved the predictive power of the coupled photosynthesis and transpiration model. The response of CO_2 flux, canopy conductance and latent heat flux to changes in climatic factors was discussed, which indicated the model could be used to predict CO_2, water and heat fluxes of wheat not only in the North China Plain, but also in other climatic regions in China.

Keywords: Photosynthesis–transpiration coupled model; CO_2 flux; Sensible and latent heat fluxes; Eddy covariance method; Winter wheat; The North China Plain

1. Introduction

Photosynthesis and transpiration are two basic processes in forming crop productivity. Accurate estimation of photosynthesis and water consumption is important not only in directing irrigation and improving water use efficiency of cropland, but also in studying the interactions between plant and atmosphere. The simulation of photosynthesis and evapotranspiration has been intensively studied in the past decades at all levels, from individual leaf, canopy and region scale to the global scale. Farquhar et al. (1980) and von Caemmerer and Farquhar (1981) proposed a biochemical model of photosynthesis for C_3 plant, which is the foundation of many large-scale models because it is mechanistically based and because it needs few parameters. Simultaneously, it is of importance to study the feedbacks between biochemical and biophysical processes of leaf response. Many researchers have

* Corresponding author. Tel.: +86 10 64856515; fax: +86 10 64851844.
E-mail address: yuq@igsnrr.ac.cn (Q. Yu).

0168-1923/$ – see front matter © 2006 Elsevier B.V. All rights reserved.
doi:10.1016/j.agrformet.2006.02.007

described the ratio of stomatal conductance of C_3 plant and CO_2 assimilation rate and their response to environmental factors (Jarvis, 1976; Ball, 1987; Ball et al., 1987; Collatz et al., 1991; Leuning, 1995; Nikolov et al., 1995). Photosynthesis models on the canopy scale are generally divided into the big leaf model and multilayer model (Baldocchi, 1992; Amthor, 1994). The big leaf model treats the canopy as an extended leaf (Farquhar, 1989; Sellers et al., 1992; Baldocchi and Harley, 1995; Norman, 1993; Kull and Jarvis, 1995). Some multilayer models deal with sunlit leaves and sunshade leaves separately (Norman, 1980; Leuning et al., 1995; Wang and Leuning, 1998; Chen et al., 1999).

Mathematical models for calculating sensible heat and latent heat fluxes can generally be classified into single-layer models, two-layer models and multilayer models. In the single-layer models, the Penman–Monteith formula (Penman, 1948; Monteith, 1965) was frequently used to estimate evapotranpsiration (Brutsaert and Stricker, 1979; Katul and Parlange, 1992; Parlange and Katul, 1992; Konzelmann et al., 1997). Two-layer models calculate canopy transpiration and soil evaporation separately (Shuttleworth and Wallace, 1985; Choudhury and Monteith, 1988; Noilhan and Planton, 1989; Kustas, 1990). Multilayer models include the effects of within canopy transfer, vertical variation in canopy structure and distributions of exchange the sources and sinks (Chen, 1984; Tanaka et al., 1998; Wu et al., 2000; Anadranistakis et al., 2000).

Photosynthesis and transpiration are interdependent and inseparable since they take place in the leaf. Many models combine photosynthesis and transpiration through a model for stomatal resistance (Collatz et al., 1991; Leuning et al., 1995; Yu et al., 2001). On calculating evapotranspiration, although single-layer models have been extensively used because of their simplicity and general applicability, they cannot be appropriately applied to arid or semi-arid lands because sources/sinks of fluxes occur at separated canopy and soil surface (Domingo et al., 1999), and the application of multilayer models are limited because the micro-meteorological variables within canopy are difficult to obtain.

From the above review, we can see that the parameterization methods on calculating photosynthesis and transpiration are complicated and often dissimilar. Therefore, it is of significance to select appropriate parameterization methods and integrate them into a model for simulating photosynthesis and evapotranspiration under various climatic and soil conditions. Thus, we developed a model that combined a two-layer evapotranspiration model with a coupled photosynthesis–stomatal model to study the diurnal variations of CO_2, water and heat fluxes of winter wheat at the canopy level based on long-term continuous measurements in ChinaFlux.

The North China Plain is one of the most important areas of agricultural production in China and the winter wheat which covers a large part of this area may contribute significantly to the CO_2, water and heat exchanges between the atmosphere and terrestrial ecosystems. Therefore, measurement and simulation of CO_2, water and heat fluxes of winter wheat is of importance to appraise the function of croplands against regional water and carbon cycles. However, there are few publications that provide a thorough description of measurements and simulations of the diurnal variation of CO_2, water and heat fluxes of winter wheat field in the North China Plain.

The objectives of this paper are as follows:

(1) To measure the diurnal variation of CO_2, water and heat fluxes of winter wheat and analyze the relation between CO_2, water and heat fluxes and environmental factors.
(2) To develop a model which couples photosynthesis and transpiration to describe the interactions of atmosphere, crop and soil in the agro-ecosystem.
(3) To test the model and perform a numerical analysis of the response of the model under variable climatic environmental conditions.

2. Model descriptions

The model consists of a canopy evapotranspiration module, a canopy photosynthesis module and a soil water and heat transfer module. Three modules were coupled by using the canopy photosynthesis model to calculate canopy resistance that was needed in the canopy evapotranspiration model, using the evapotranspiration model to obtain soil temperature and canopy temperature to calculate photosynthetic rate and soil respiration. Simultaneously, the canopy evapotranspiration model was combined with the water and heat transfer model in the soil to solve energy balance equations.

2.1. Canopy evapotranspiration model

The canopy evapotranspiration model includes a solar radiation transfer submodel, a thermal radiation

submodel, a two-layer water and heat transfer submodel and a resistance submodel.

2.1.1. Solar radiation transfer submodel

The global radiation above the canopy is divided into the direct visible radiation (S_{dv}), the direct infrared radiation (S_{di}), the diffuse visible radiation (S_{sv}) and the diffuse infrared radiation (S_{si}). Light intensity (I) inside the canopy decreased exponentially with the leaf area index according to Beer's law. That is:

$$I = I_0 e^{-\eta L} \tag{1}$$

in which I_0 is the light intensity at the top of canopy, η the extinction coefficient and L is the leaf area index (see Appendix B for a full list of symbols). Because the extinction coefficient and albedo of canopy for direct radiation and diffuse radiation are different, they are calculated separately in the model (see Appendix A.1).

2.1.2. Thermal radiation submodel

The radiation balance equation of ground surface is given by:

$$R_n = (1 - \rho_a)R_g - F_n \tag{2}$$

in which R_n is the net radiation above the canopy, ρ_a the albedo of canopy and soil to solar radiation, R_g the global radiation and F_n is surface effective radiation. The radiation balance equations of soil and canopy are calculated by the following equations:

$$\begin{aligned} R_{ns} = {} & S_{dv}(1 - \rho_v)e^{-k_v L} + S_{di}(1 - \rho_i)e^{-k_i L} \\ & + S_{sv}(1 - \rho_{dv})e^{-k_{dv} L} + S_{si}(1 - \rho_{di})e^{-k_{di} L} - R_{ls} \end{aligned} \tag{3}$$

and

$$\begin{aligned} R_{nc} = {} & S_{dv}(1 - \rho_v)(1 - e^{-k_v L}) + S_{di}(1 - \rho_i)(1 - e^{-k_i L}) \\ & + S_{sv}(1 - \rho_{dv})(1 - e^{-k_{dv} L}) + S_{si}(1 - \rho_{di}) \\ & \times (1 - e^{-k_{di} L}) - R_{lc} \end{aligned} \tag{4}$$

in which R_{ns} and R_{nc} are the net radiation absorbed by the soil and by the canopy, respectively. R_{ls} is long wave radiation of soil and R_{lc} is long wave radiation of the canopy. ρ_v, ρ_i, ρ_{dv} and ρ_{di} are albedo of canopy for direct visible radiation, direct infrared radiation, diffuse visible radiation and diffuse infrared radiation, respectively. k_v, k_i, k_{dv} and k_{di} are the extinction coefficient of canopy for direct visible radiation, direct infrared radiation, diffuse visible radiation and diffuse infrared radiation, respectively.

2.1.3. Two-layer water and heat transfer submodel

The energy balance equation of cropland, not considering the effects of advection, is given by:

$$R_n = H + \lambda E + G \tag{5}$$

in which H, λE and G are sensible heat flux above the canopy, latent heat flux above the canopy and soil heat flux, respectively. The energy balance equations of canopy and soil are expressed by:

$$R_{nc} = H_c + \lambda E_c \tag{6}$$

$$R_{ns} = H_s + \lambda E_s + G \tag{7}$$

in which H_c and H_s are the sensible heat fluxes of canopy and soil, respectively, and λE_c and λE_s are the latent heat fluxes of canopy and soil, respectively. Then soil evaporation and crop transpiration are given by (see Appendix A.2):

$$\lambda E_c = \frac{\Delta(R_n - R_{ns}) + \rho C_p D_0 / r_a^c}{\Delta + \gamma(1 + r_s^c / r_a^c)} \tag{8}$$

$$\lambda E_s = \frac{\Delta(R_{ns} - G) + \rho C_p D_0 / r_a^s}{\Delta + \gamma(1 + r_s^s / r_a^s)} \tag{9}$$

The sensible heat fluxes of canopy and soil are estimated by the following expressions:

$$H_s = \rho C_p \frac{T_s - T_a}{r_a^a + r_a^s} \tag{10}$$

$$H_c = \rho C_p \frac{T_c - T_a}{r_a^a + r_a^c} \tag{11}$$

in which ρ is the air density, C_p the specific heat of air at constant pressure, λ the latent heat of vaporization, Δ the slope of saturation vapor press at air temperature, γ the psychometric constant, D_0 the saturation deficit at canopy source height, T_a the air temperature at reference height, r_a^a the aerodynamic resistance between the canopy source height and reference height, r_a^c the boundary layer resistance of canopy, r_a^s the aerodynamic resistance between the substrate and canopy source height, r_s^c the canopy resistance and r_s^s is the soil resistance.

Soil surface temperature and canopy temperature are calculated by iteration in the model. The initial values of canopy temperature and soil surface temperature are given to the model, and then sensible heat fluxes of canopy and soil are calculated with Eqs. (10) and (11). The values thus obtained are used in the energy balance equation and the iteration is continued until the difference between the sum of sensible and latent heat fluxes of canopy and net radiation of the canopy is

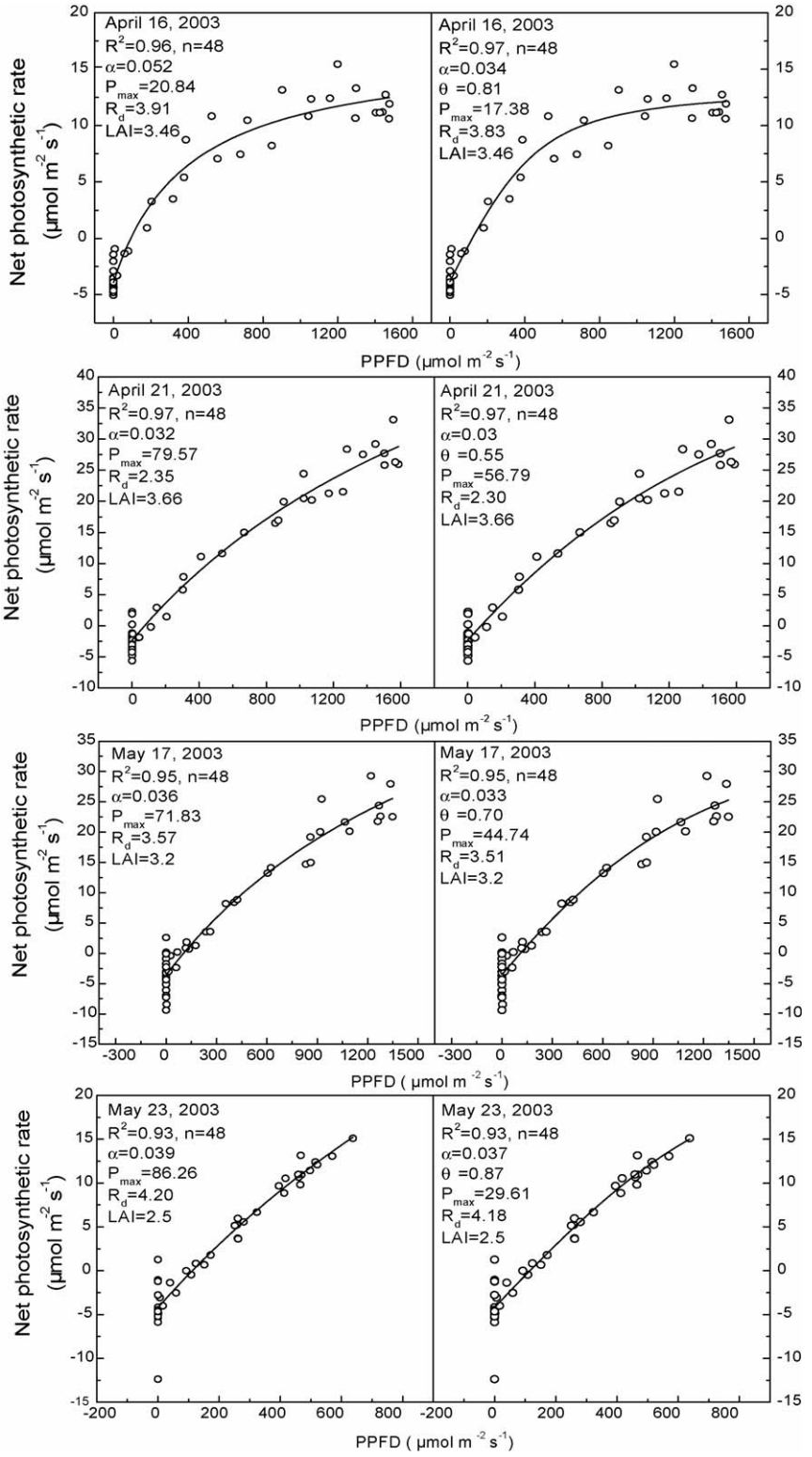

Fig. 1. The response curve of canopy net photosynthetic rate to photosynthetic photo flux density (PPFD) (left is a rectangular hyperbola and right is a non-rectangular hyperbola).

<0.1 W m^{-2}. Similarly, the iteration is done until the difference between the sum of sensible and latent heat fluxes of soil and net radiation absorbed by soil is <0.1 W m^{-2}. Then sensible heat fluxes of the canopy and soil are obtained by Eqs. (10) and (11) from canopy temperature and soil temperature and latent heat fluxes of canopy and soil are obtained with Eqs. (8) and (9).

2.1.4. The resistance submodel

Determination of the resistances is important to solve the energy balance equation. Aerodynamic resistance, boundary layer resistances of canopy, canopy resistance and soil resistance need to be calculated in the model. Soil resistance is calculated with an empirical function dependent on surface soil water content and it is described in the model (Lin and Sun, 1983):

$$r_s^s = b_1 \left(\frac{\theta_s}{\theta} \right)^{b_2} + b_3 \tag{12}$$

in which θ is the average soil water content between 0 and 10 cm, θ_s the saturated water content of surface soil and b_1, b_2 and b_3 are the empirical constants. Crop and soil are considered as a unique aerodynamic system, the characteristics of which are expressed by the values of zero plane displacement (d) and roughness length (z_0), given by the expressions (Mehrez et al., 1992):

$$d = 0.63\sigma_\alpha h \tag{13}$$

$$z_0 = (1 - \sigma_\alpha) z_b + \frac{\sigma_\alpha (h - d)}{3} \tag{14}$$

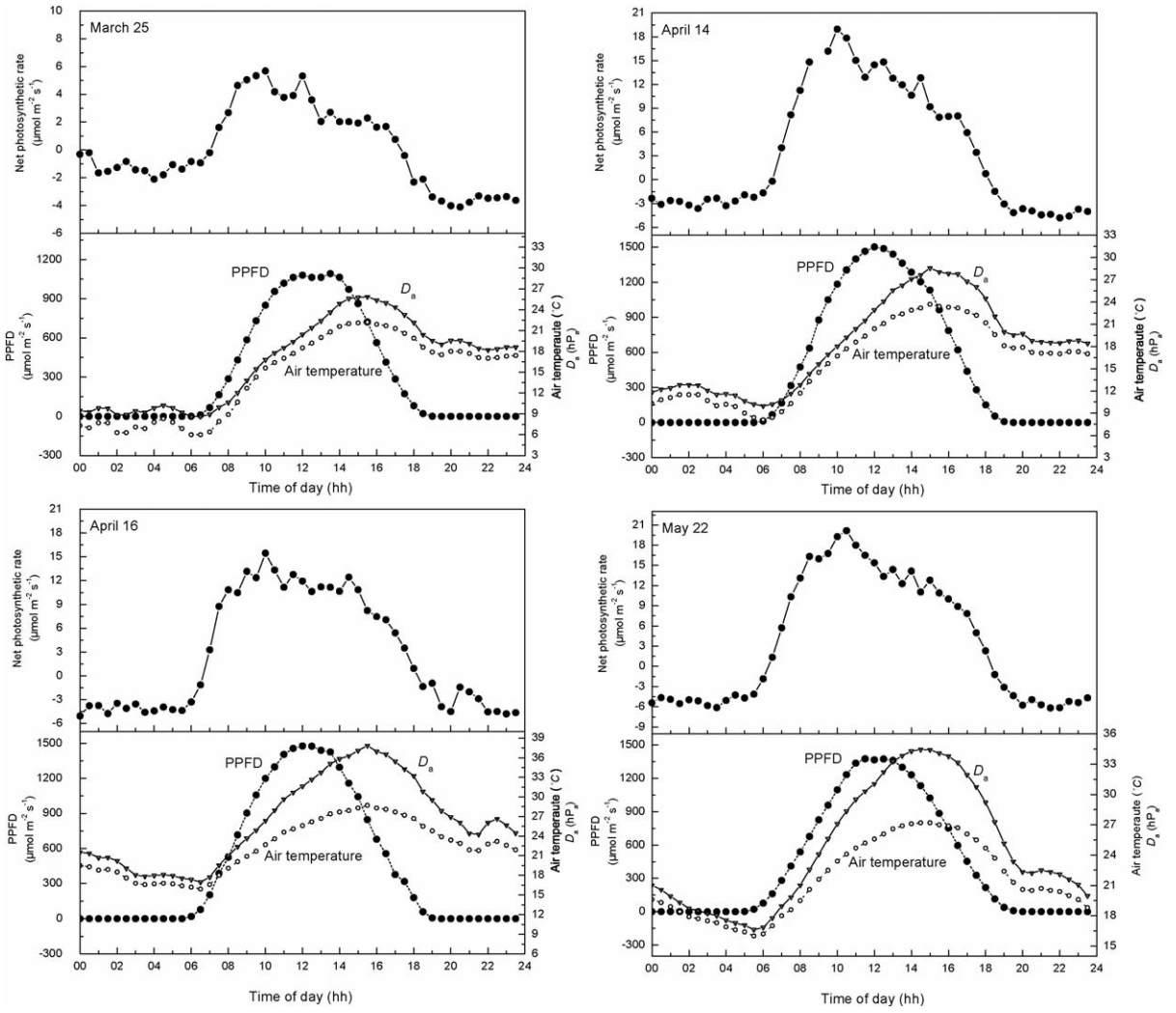

Fig. 2. Diurnal variation of weather variables (PPFD, D_a and air temperature) and canopy net photosynthetic rate on several typical cloudless days.

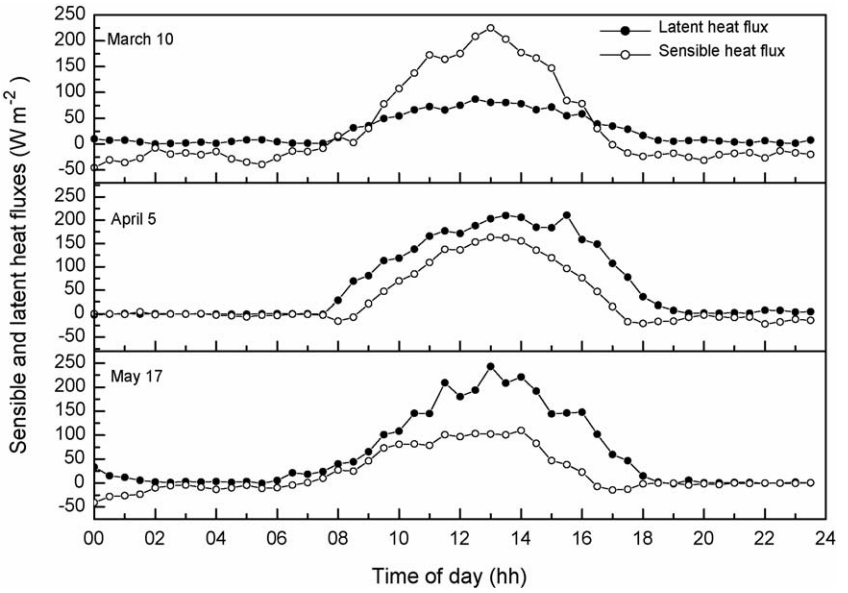

Fig. 3. Diurnal variations of sensible and latent heat fluxes on typical clear days.

in which h is the crop height, z_b the roughness length of bare soil, usually taking the value 0.01 m (Van Bavel and Hillel, 1976) and σ_α is the momentum partition coefficient which depends on leaf area index (L) expressed as (Shaw and Pereira, 1981):

$$\sigma_\alpha = 1 - \left(\frac{0.5}{0.5+L}\right)\exp\left(-\frac{L^2}{8}\right) \quad (15)$$

r_a^c, r_a^a and r_a^s can be expressed as fractions of the overall aerodynamic resistance for momentum transfer in the soil–vegetation system (r_a) (Anadranistakis et al., 1999):

$$r_a^c = \frac{u_h}{\sigma_\alpha u_*^2} = \frac{u_h}{\sigma_\alpha u_r} r_a \quad (16)$$

$$r_a^a = \frac{u_r - u_h}{u_*^2} = \frac{u_r - u_h}{u_r} r_a \quad (17)$$

$$r_a^s = \frac{u_h}{(1-\sigma_\alpha)u_*^2} = \frac{u_h}{(1-\sigma_\alpha)u_r} r_a \quad (18)$$

in which u_* is the friction velocity, u_r the wind speed at the reference height and r_a is the function of atmospheric stability and can be expressed by:

$$r_a = \frac{1}{k^2 u(z)}\left[\ln\frac{z-d}{z_0} - \psi_M\right]\left[\ln\frac{z-d}{z_0'} - \psi_H\right] \quad (19)$$

where k is the von Karman's constant, $z_0' = z_0/7$ (Garratt, 1978). Here we assumed atmosphere is under neutral stability conditions, thus $\psi_M = \psi_H = 0$, and wind speed at mean canopy height is described by:

$$u_h = 0.83u(z)\sigma_\alpha + (1-\sigma_\alpha)u_r \quad (20)$$

Canopy resistance to water vapor is a reciprocal of canopy conductance which is the sum of conductance of sunlit ($g_{sw,n}$) leaves and sunshade leaves ($g_{sw,e}$):

$$r_s^c = \frac{1}{g_{sw,n} + g_{sw,e}} \quad (21)$$

The calculation of leaf stomatal conductance is given in Appendix A.4.

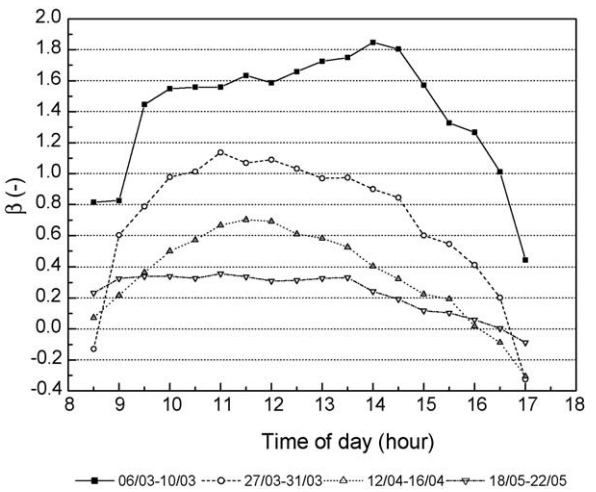

Fig. 4. The day-time patterns of Bowen ratio (β) during four different development stages (average value of every 5 days).

2.2. Canopy photosynthesis model

Canopy net photosynthetic rate is the sum of net photosynthetic rate of sunlit leaves ($A_{nc,n}$) and shaded leaves ($A_{nc,e}$),

$$A_{nc} = A_{nc,e} + A_{nc,e} \quad (22)$$

Leaf net photosynthetic rate is the difference between leaf gross photosynthetic rate (A) and leaf dark respiration (R_d),

$$A_n = A - R_d \quad (23)$$

The calculations of A and R_d, see Appendix A.3.

Soil respiration (R_s) is calculated as a function of soil temperature using:

$$R_s = R_0 Q_{10}^{(T_s-25)/10} \quad (24)$$

in which R_0 is the soil respiration at reference temperature, T_s the average soil temperature between 0 and 10 cm and Q_{10} is the temperature constant. The CO_2 flux above the canopy (F_c) is given by the follow expression:

$$F_c = A_{nc} - R_s \quad (25)$$

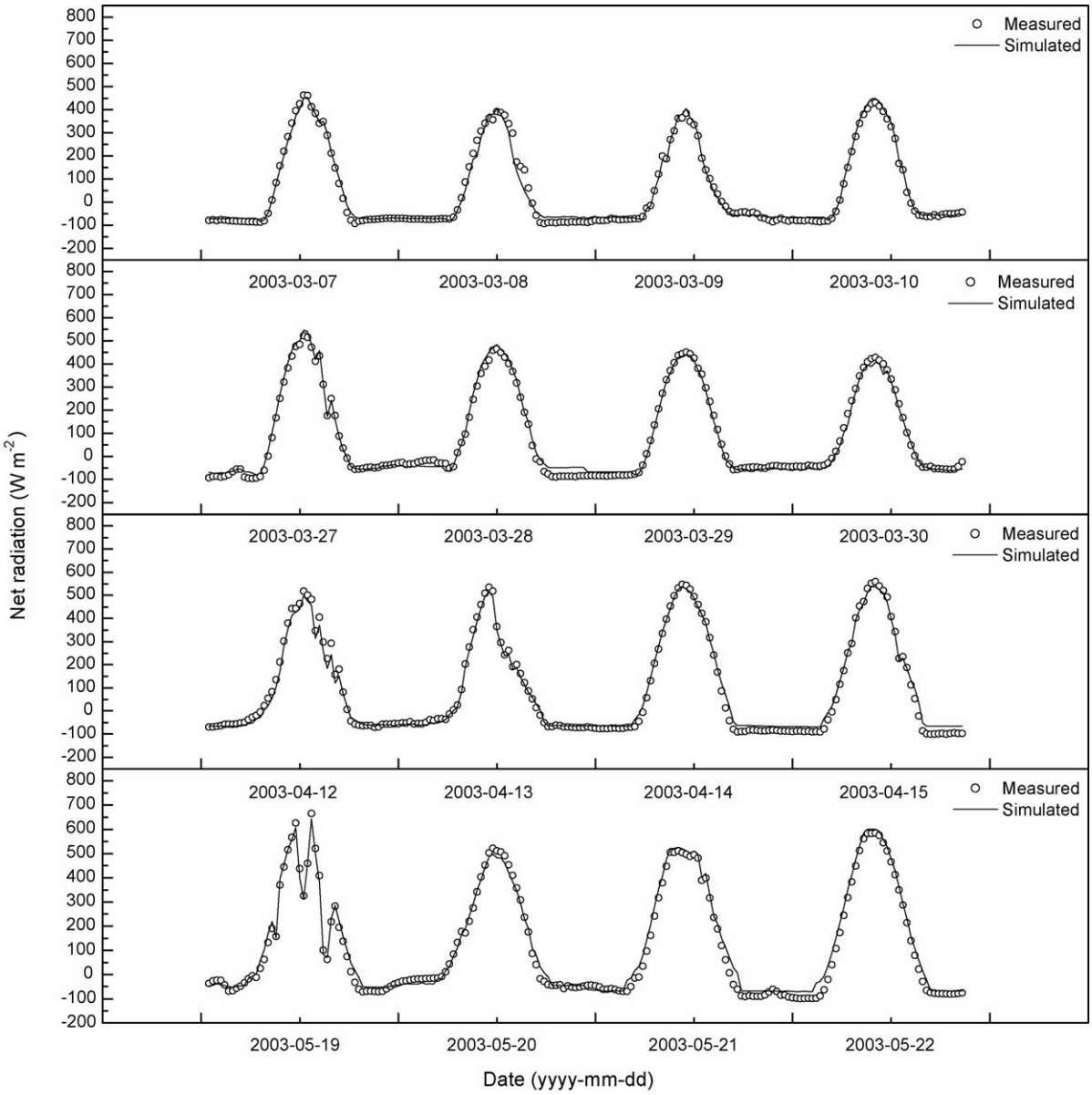

Fig. 5. Comparison between simulated and measured net radiation above winter wheat canopy at four development stages.

2.3. The model for soil water and heat transfer

2.3.1. Soil water movement submodel

The soil is divided into several layers, and vertical water movement in it is described by:

$$D_1 \frac{d\theta}{dt} = P_1 + I_1 - E_s - Q_{1,2} - S_1 \quad (26)$$

$$D_i \frac{d\theta_i}{dt} = Q_{i-1,i} - Q_{i,i+1} - S_i \quad (27)$$

$$D_n \frac{d\theta_n}{dt} = Q_{n-1,n} - Q_n - S_n \quad (28)$$

in which i is the layer number ($i = 2, \ldots, n$), D the layer thickness, θ the volume water content of the soil, Q the water flux through the ith layer and $(i + 1)$th layer interface between two adjacent compartments, with downward flux taken as positive and S is the absorption rate of roots. P_1 and I_1 are intensities of precipitation and irrigation, respectively. E_s is the soil evaporation rate and t is the time.

2.3.2. Root water uptake submodel

Feddes and Zaradny (1978) proposed a water absorption model for roots by taking account of a weighting factor of soil water potential. The water absorption rate (S) was expressed by the function of the transpiration rate, root length and soil water potential:

$$S_i = \frac{\alpha(\psi_i)}{\int_0^{L_r} \alpha(\psi_i)\, dz} T_r \quad (29)$$

in which ψ_i is the soil water potential at layer i, L_r the root length, T_r the transpiration rate and $\alpha(\psi_i)$ is the weighting factor of soil water potential and is

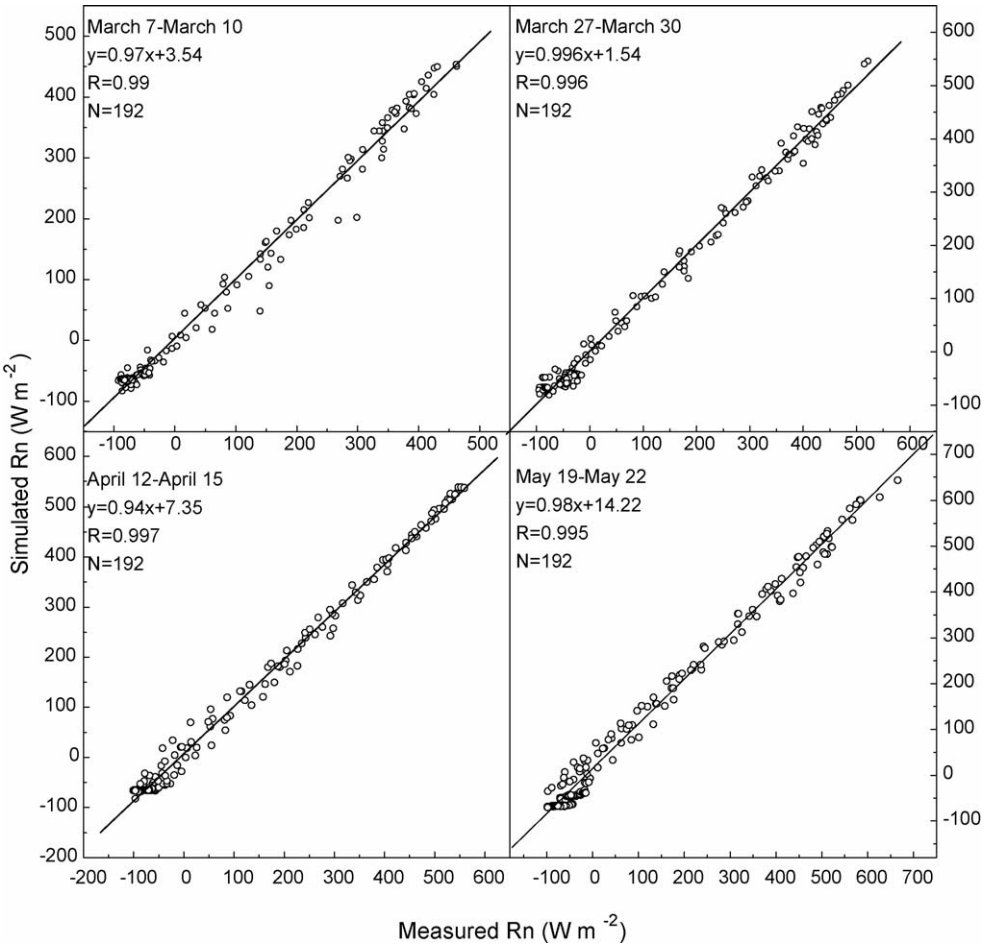

Fig. 6. Correlation analysis of simulated and measured net radiation (R_n) at four development stages.

defined as:

$$\alpha(\psi) = \begin{Bmatrix} \dfrac{\psi}{\psi_1} & \psi_1 \le \psi \le 0 \\ 1 & \psi_2 \le \psi < \psi_1 \\ \dfrac{\psi - \psi_3}{\psi_2 - \psi_3} & \psi_3 \le \psi < \psi_2 \\ 0 & \psi < \psi_3 \end{Bmatrix} \quad (30)$$

in which ψ_1, ψ_2 and ψ_3 are thresholds of soil water potential for the three levels. This soil water model is suitable for root absorption $\alpha(\psi) = 1$ when its potential ranges from ψ_1 to ψ_2, and $\alpha(\psi)$ are lower than 1 when water potentials is lower than ψ_2 or higher than ψ_1 due to drying or excess water and low aeration. Soil water is not available for root when its potential is lower than ψ_3.

2.3.3. Heat diffusion equation submodel

The heat diffusion equation for heterogeneous soil can be expressed by:

$$c(z)\frac{\partial T}{\partial t} = \frac{\partial}{\partial z}\left(K(z)\frac{\partial T}{\partial z}\right) \quad (31)$$

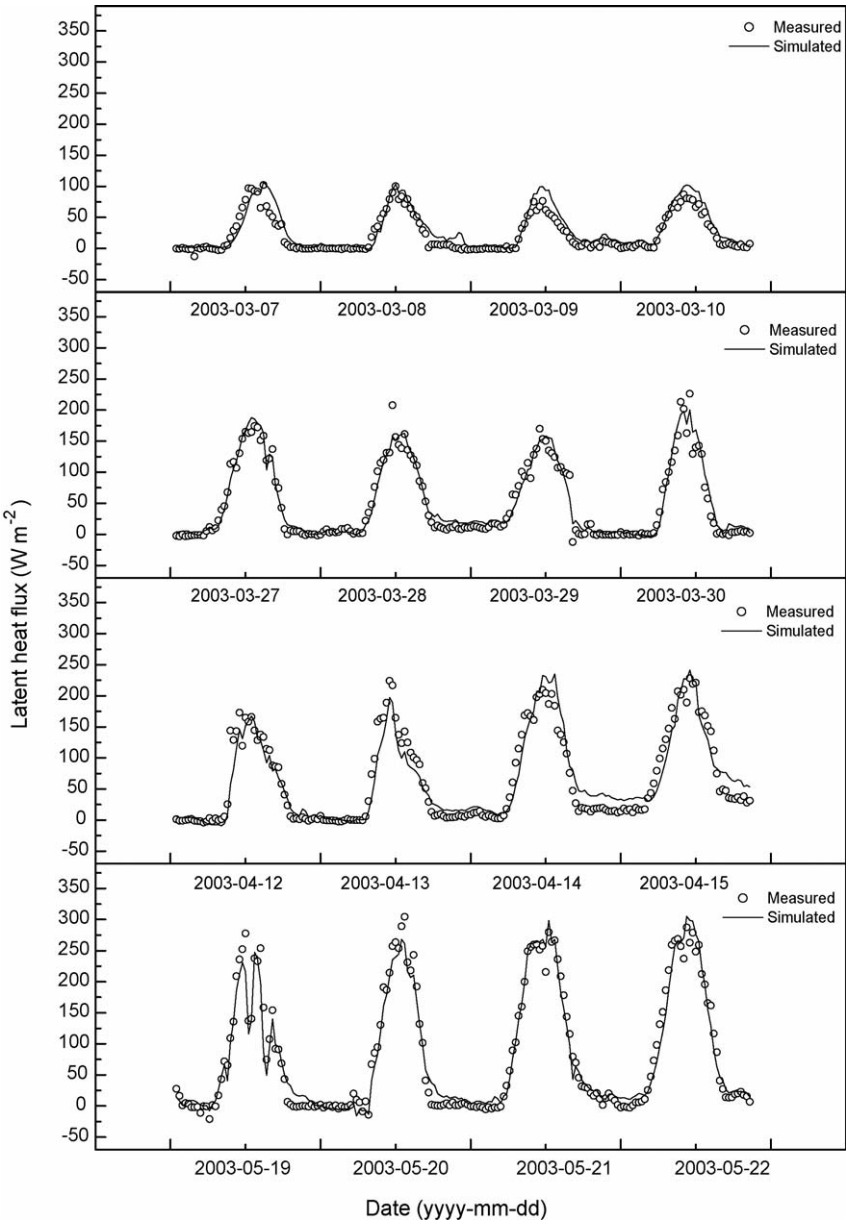

Fig. 7. Comparison between the simulated and the measured values of latent heat flux above winter wheat canopy at four development stages.

in which $c(z)$ is the specific heat of soil at depth z and $K(z)$ is the soil heat conductivity at depth z. The heat diffuse equation can be solved by implicit difference scheme of integration. Soil heat flux at depth z is described by:

$$G = -K(z)\frac{\partial T}{\partial z} + \int_0^z \frac{\partial T}{\partial t} c(z)\,\mathrm{d}z \tag{32}$$

Under many conditions the effect of $\int_0^z (\partial T/\partial t)c(z)\,\mathrm{d}z$ for soil heat flux can be neglected (Leyton, 1975), then soil heat flux through the ground surface can be calculated with difference method,

$$G = -K(z)\left[\frac{T_\mathrm{g} - T_\mathrm{s}}{\Delta z}\right] \tag{33}$$

in which T_g is the soil surface temperature, T_s the average temperature from surface ground to depth z.

3. Materials and methods

The experiments were conducted at Yucheng Comprehensive Experiment Station in the North China Plain (36°40′N, 116°22′E, 28 m above m.s.l) in 2002–2003, which is a cropland site of ChinaFlux. The annual mean air temperature was 13.1 °C and mean temperature in January and July were −3 and 26.9 °C, respectively. The mean annual precipitation was 610 mm and nearly 70% of it was concentrated in summer. The dominant soil type is silty loam with an average bulk density of 1.28 g cm^{-3}. The cropping system in the region is summer maize followed by winter wheat. There is a fetch of over 500 m for winds from all directions at each site in the growing season of winter wheat and maize.

Fluxes of CO_2, sensible and latent heat were measured with an eddy covariance system installed at 2.10 m above the ground. The system consisted of a fast

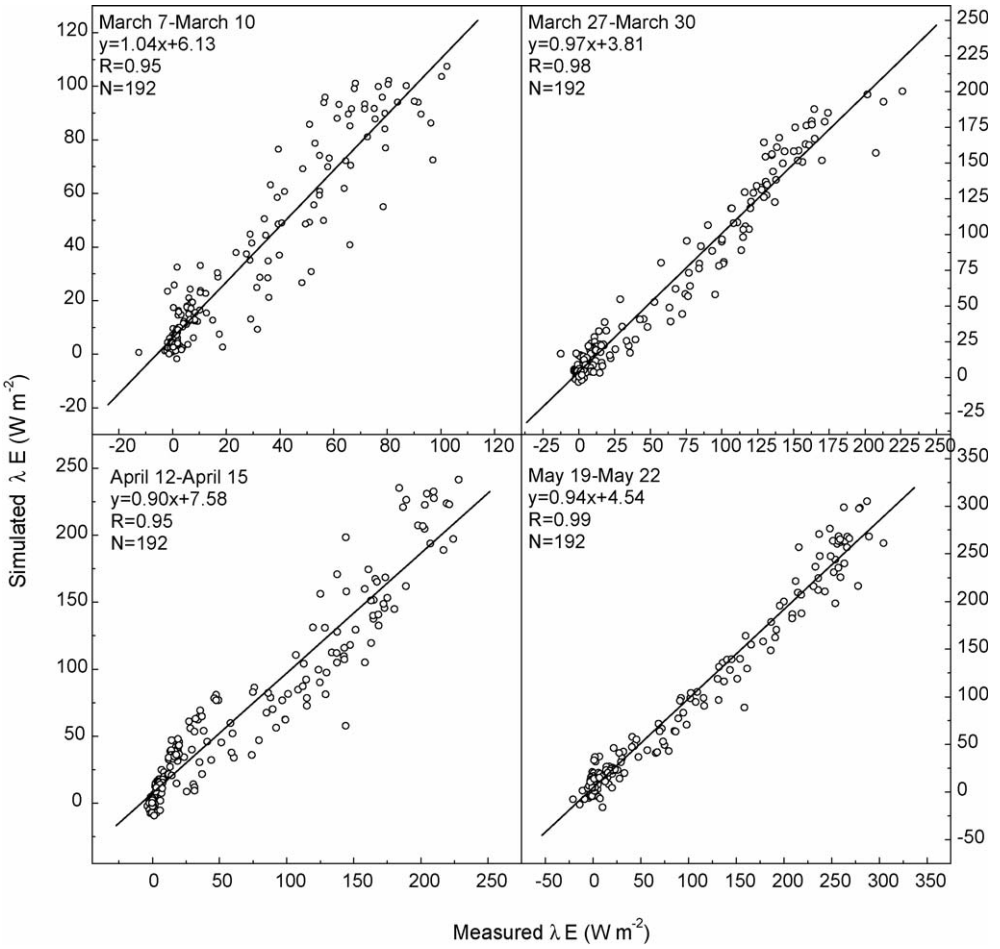

Fig. 8. The correlation analysis of simulated and measured latent heat flux (λE) above winter wheat canopy at four development stages.

response infrared gas analyzer (LI7500, LI-COR Inc.) and a three-dimension sonic anemometer (CSAT3, Campbell Scientific Inc.). Data were recorded with a data-logger (CR23X CSI) and the sampling frequency was 20 Hz for all each channel. The average values were calculated and recorded every 30 min.

A radiometer (CNR1, Kipp&Zonen) was installed at 1.68 m above the ground to measure downward and reflected components of shortwave and longwave radiation. Air temperature and relative humidity were measured with temperature/humidity probes (HMP45C, VAISALA). Wind speed was measured with an anemometer (A100R, Vector). Two heat flux plates (HFP01SC, Hukseflux) was set at 0.05 m below the ground at row and aisle position to measure soil heat flux. More information on micrometeorological measurements and data processes at this site can be found in other papers in this special issue.

During each development stage, 50 plants were randomly harvested and the length and width of each leaf were measured and the leaf area index was calculated by combing average area for leaf, number of leaves per plant and the plant density. Soil water content was measured every 5 days by weighing; readings were

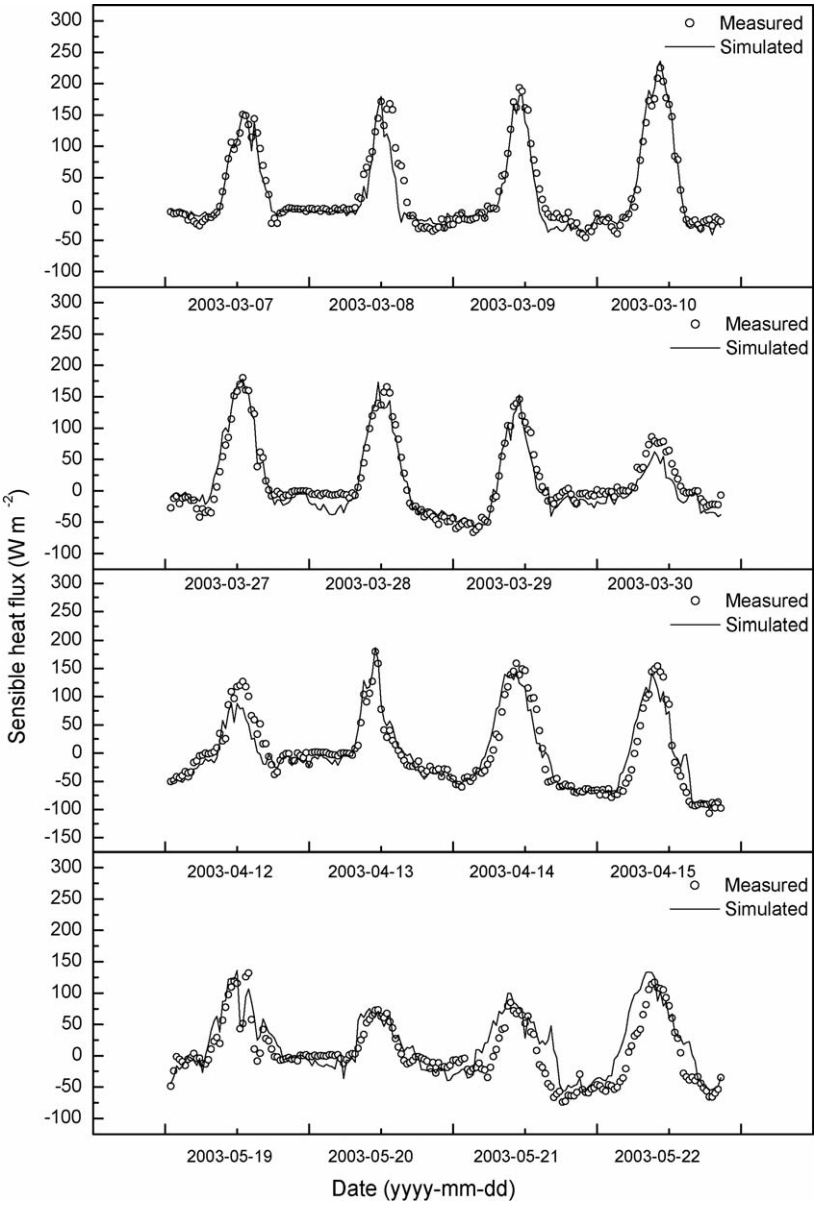

Fig. 9. Comparison between simulated and measured values of sensible heat flux above winter wheat canopy at four development stages.

taken to calculate the average water content of every layer in 10 cm increments over a depth of 100 cm.

4. Results and discussion

4.1. Diurnal variation of CO_2 flux above the canopy

4.1.1. The response of CO_2 flux above the canopy to PPFD

Fig. 1 shows some typical light response curves of canopy net photosynthetic rate. The relation between canopy net photosynthetic rate and photosynthetic photon flux density (PPFD) can be expressed as a rectangular hyperbola or a non-rectangular hyperbola, and both can simulate the relation very well with $R^2 > 0.9$. The results show that solar radiation is the main factor affecting canopy net photosynthetic rate. In general, canopy net photosynthetic rate increases with an increase in PPFD, but excessively high light intensities may lead to photoinhibition. This did not occur during the growing season of winter wheat because PPFD was always <1600 μmol m^{-2} s^{-1} in the North China Plain. The light response curves differ with development stages, which show that other environmental factors also play a significant role in determining the diurnal variation of canopy net photosynthetic rate.

4.1.2. Midday depression of canopy photosynthesis of winter wheat

Midday depression of photosynthesis is a common phenomenon for many crops under natural condition. One of the reasons is limited soil moisture (Tazaki et al., 1980; Tuzet et al., 2003). But even when soil moisture is adequate, photosynthesis may decrease at midday and in the afternoon (Larson et al., 1981; Ishihara and Saito, 1987; Pettigrew et al., 1990; Hirasawa and Hsiao, 1999).

Diurnal changes of weather variables and canopy net photosynthesis rate on several typical cloudless days are presented in Fig. 2. On March 25, the lowest air temperature (6 °C) occurred at 06:00 h, and increased

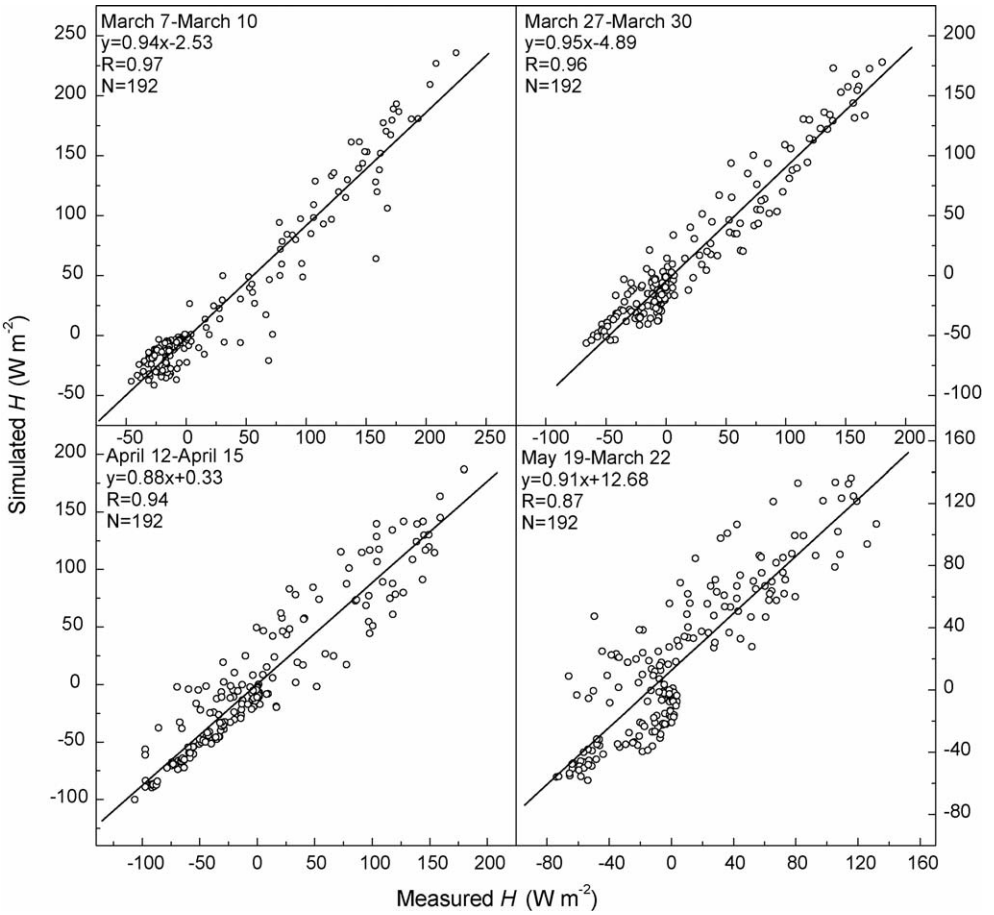

Fig. 10. Correlation analysis of simulated and measured sensible heat flux (H) above winter wheat canopy at four development stages.

over the daytime with solar radiation and reached the highest value of 22 °C at 15:00 h. The trend of change in air water vapor saturation deficit (D_a) was similar to air temperature with a lowest value of 8.6 h Pa at 06:00 h and a maximal value of 25.9 h Pa at 15:00 h. Canopy net photosynthetic rate was low in the morning and reached a maximum of 5.7 μmol m^{-2} s^{-1} at 10:00 h, and decreased for the rest of the day. On May 22, D_a was 16.6 h Pa at 05:00 h and the highest D_a was 34.5 h Pa at 14:30 h. Canopy net photosynthetic rate reached a maximum value of 20.2 μmol m^{-2} s^{-1} at 10:30 h and decreased sharply, though PPFD was as high as 1500 μmol m^{-2} s^{-1} at midday. Fig. 2 shows that there was a lowering of photosynthesis from before midday and in the afternoon. It may be caused by stomatal closure due to high D_a and canopy temperature which was supported by many studies (Hirasawa et al., 1989; Pettigrew et al., 1990). Tuzet et al. (2003) and Leuning et al. (2004) provided a more thorough explanation of the midday depression of photosynthesis. Stomatal conductance depends on not only light, temperature and intercellular CO_2 concentration via photosynthesis but

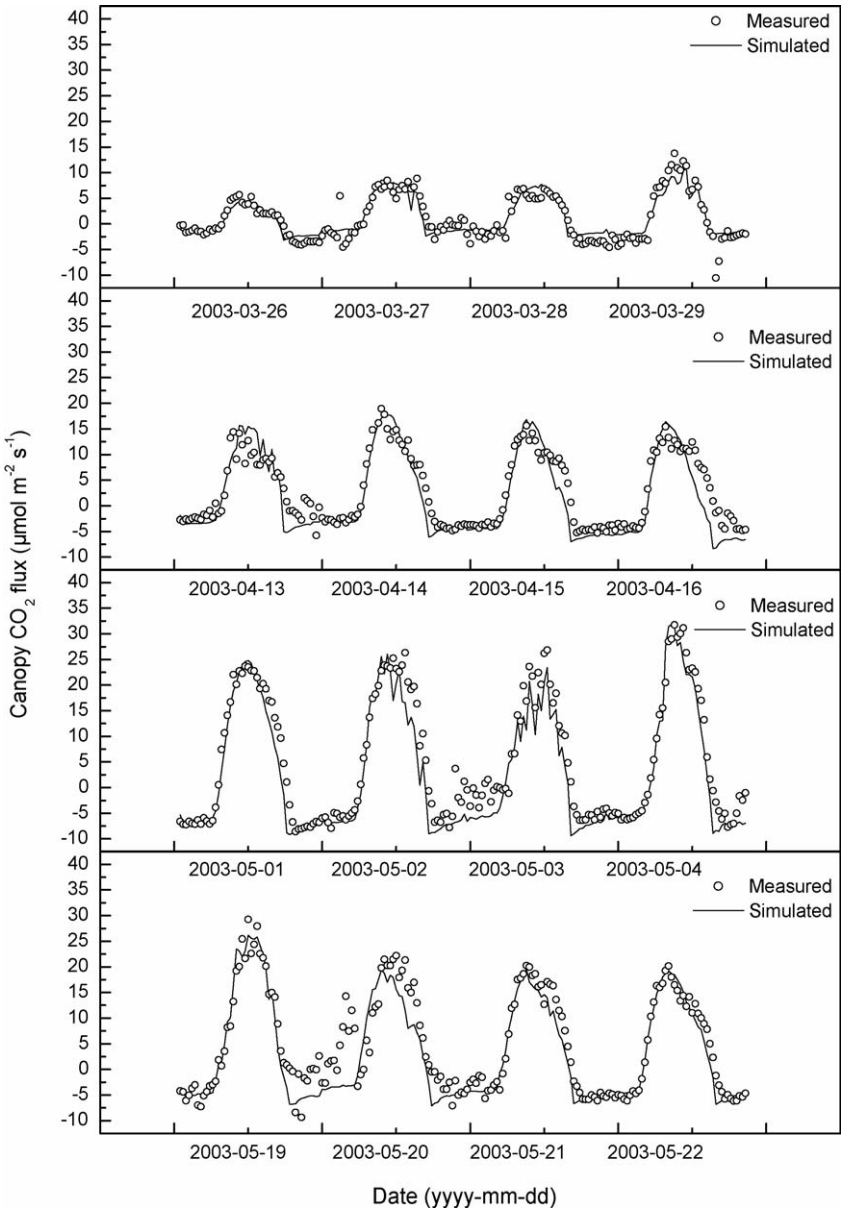

Fig. 11. Comparison between simulated and measured values of CO_2 flux above winter wheat canopy at four development stages.

also leaf water potential, which in turn is a function of soil water potential and the rate of water flow through the soil and plant. As soil begins to dry, there is an evident midday depression of photosynthesis due to the lower leaf water potentials in the noon and the afternoon than in the morning, resulting from a higher atmospheric demand and a reduced ability of the soil to supply water to the roots.

4.2. Characteristic of the diurnal variation of sensible and latent heat fluxes

The diurnal variation in sensible and latent heat fluxes over winter wheat on typical fine days are presented in Fig. 3. On March 10, sensible and latent heat fluxes were low in the morning, increased with time and reached the highest values 225 and 81 W m^{-2} at 13:00 h, respectively. On May 17, latent heat flux was larger than sensible heat flux, with a peak value of 243 W m^{-2} at 13:00 h.

Fig. 4 shows the observed diurnal variation of Bowen ratio ($\beta = H/\lambda E$) for four different development stages. Bowen ratio data were selected between 08:00 and 17:00 h because flux values at night and at sunrise or sunset are often incorrect due to small or changing temperature gradients. As can be seen in Fig. 4, the Bowen ratio increases sharply in the morning and retains a higher value from 10:00 to 15:00 h, and then decreases to a small value and sometimes even negative. Moreover, the diurnal variation of the Bowen ratio decreases with canopy development and shifts to values below unity.

4.3. Tests of the model

The main input data included air temperature, water vapor pressure, wind speed, global radiation, duration of sunshine and precipitation/applied irrigation water. Crop height and leaf area index were interpolated to daily scale resolution. The main outputs of the model are net radiation, CO_2 flux, sensible and latent heat flux.

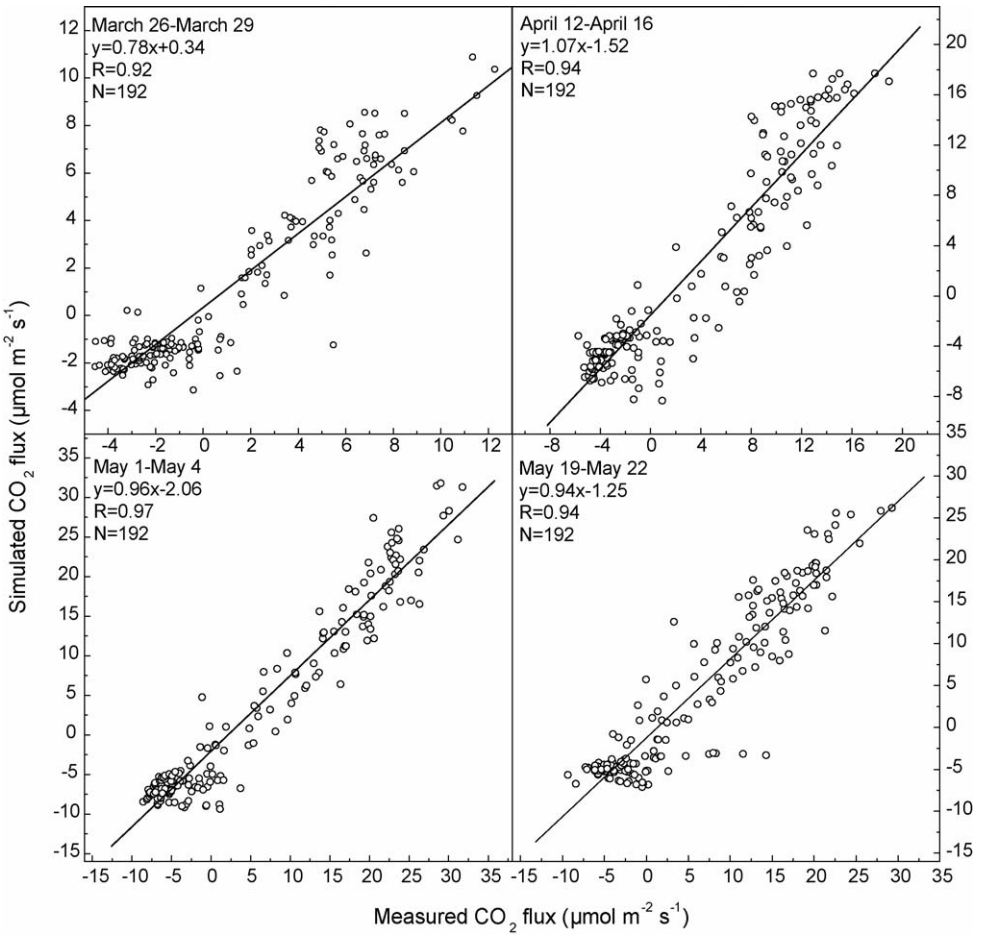

Fig. 12. Correlation analysis of simulated and measured CO_2 flux above winter wheat canopy at four development stages.

We verified the model by comparing the measured values and the simulated values. The key values and sources of parameters and constants used in the model are given Table 1.

4.3.1. Comparison between measured and simulated values of net radiation, sensible heat and latent heat fluxes above the canopy

Figs. 5 and 6 show the plots of simulated values of net radiation (R_n) above winter wheat canopy obtained by solving the radiation balance equation compared with the measured values at four development stages (March 7–10, March 27–30, April 12–15 and May 19–22). The measured and the simulated net radiation are in good agreement with correlation coefficients and regression slopes close to one and small intercepts (Fig. 6).

The comparisons of simulated and measured half-hourly data of sensible heat and latent heat fluxes at four development stages with different leaf area index are presented in Figs. 7–10. Sensible and latent heat fluxes are calculated from a two-layer evapotranspiration model. The high correlation between the measured and simulated values shows that the model does well in simulating the diurnal variations of the sensible and latent heat fluxes. As one can see from Figs. 7 and 9, sensible heat fluxes were larger than the latent heat fluxes on March 7–10 and March 27–30 when leaf area index was lower than 1.5. With an increase in leaf area index, latent heat flux became the dominant part of heat fluxes on April 12–15 and May 19–22.

4.3.2. Comparison between measured and simulated values of CO_2 fluxes above the canopy

Figs. 11 and 12 show the comparison of simulated and measured half-hourly CO_2 fluxes at different development stages (March 26–29, April 13–16, May

Table 1
The key parameters in the model

Symbol	Name	Value	Q_{10}	Source
a_1	Constant in Eq. (A3.9)	220 kJ mol^{-1}		Collatz et al. (1991)
a_2	Constant in Eq. (A3.9)	703 J mol^{-1} K^{-1}		Collatz et al. (1991)
b_1	Empirical constant in Eq. (12)	3.5		Lin and Sun (1983)
b_2	Empirical constant in Eq. (12)	2.3		Lin and Sun (1983)
b_3	Empirical constant in Eq. (12)	33.5 s m^{-1}		Lin and Sun (1983)
C_a	Ambient CO_2 concentration	350 μmol mol^{-1}		This study
C_p	Specific heat of air at constant pressure	1013 J kg^{-1} K^{-1}		Jensen et al. (1990)
I_m	Maximal light intensity in Eq. (A3.7)	4000 μmol m^{-2} s^{-1}		Yu et al. (2002)
k	von Karman's constant	0.4		Brutsaert (1988)
K_{o25}	Michaelis–Menten kinetic parameter for O_2	40×10^{-2} mol mol^{-1}		Nikolov et al. (1995)
K_{c25}	Michaelis–Menten kinetic parameter for CO_2	27×10^{-5} mol mol^{-1}		Nikolov et al. (1995)
m	Slope parameter in stomatal model in Eq. (A4.1)	8		Collatz et al. (1991)
m_1	Empirical constant in Eq. (A4.2)	2.36		This study
O	Partial pressure of O_2	20.9 kPa		Collatz et al. (1991)
R_{s0}	Soil respiration at 25 °C	0.11 mg m^{-2} s^{-1}	1.7	Yu et al. (2002)
r	Dark respiration parameter	0.015		Collatz et al. (1991)
V_{m25}	V_m^0 at 25 °C	55 μmol m^{-2} s^{-1}	2.4	Yu et al. (2002)
D_0	Parameter of humidity response	1.5 kPa		Leuning (1995)
z	Reference height	2.05 m		This study
z_b	Roughness of bare soil surface	0.01 m		Van Bavel and Hillel (1976)
α	Intrinsic quantum efficiency	0.06		Yu et al. (2002)
β_1	Convexity coefficient	0.95		Collatz et al. (1991)
β_2	Convexity coefficient	0.98		Collatz et al. (1991)
γ	Psychrometric constant	0.67 h Pa K^{-1}		Goudriaan (1977)
ψ_1	Thresholds of soil water potential in Eq. (30)	−0.3 m		Luo et al. (2001)
ψ_2	Thresholds of soil water potential in Eq. (30)	−6 m		Luo et al. (2001)
ψ_3	Thresholds of soil water potential in Eq. (30)	−15 m		Luo et al. (2001)
σ	Stefan-Boltzmann constant	5.668×10^{-8} W m^{-2} K^{-4}		Goudriaan (1977)
σ_l	Leaf scattering coefficient	0.2 for VIS; 0.8 for NIR		Norman (1985)
λ	Latent heat of vaporization for water	2.46×10^6 J kg^{-1}		Brutsaert (1988)
θ_f	Saturated soil water content	0.40 m^3 m^{-3}		Measured in field
θ_s	Saturated soil water content	0.35 m^3 m^{-3}		Measured in field
θ_w	Saturated soil water content	0.13 m^3 m^{-3}		Measured in field
ρ	Bulk density	1.28 g m^{-3}		Measured in field

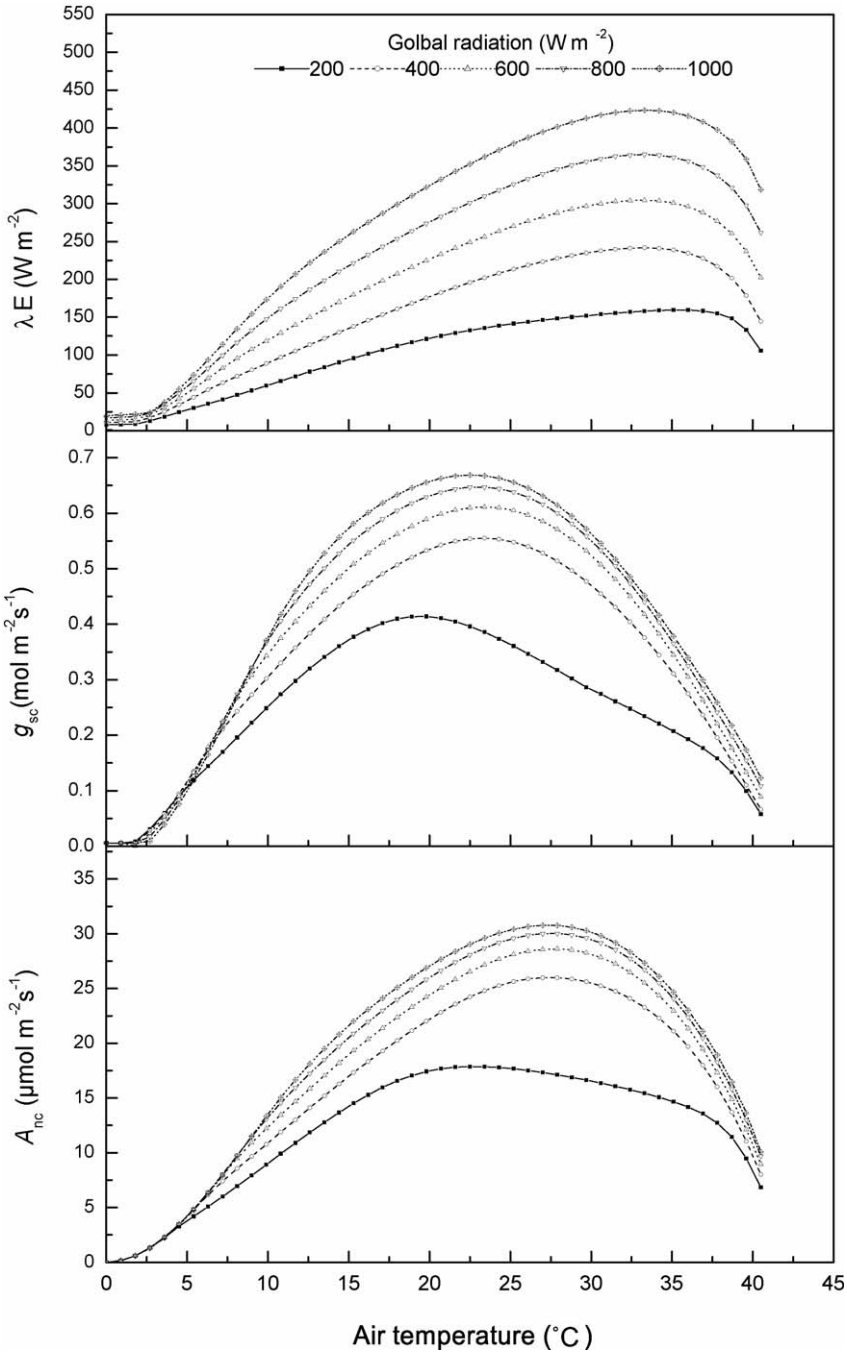

Fig. 13. The response of latent heat flux (λE), canopy conductance (g_{sc}) and canopy net photosynthetic rate (A_{nc}) of winter wheat to the change in air temperature (0–45 °C) at five irradiance levels at relative humidity, 60% and wind speed, 2 m s^{-1}.

1–4 and May 19–22). The simulated CO_2 fluxes are in good agreement with measured values with regression slopes near one and small intercepts. The high correlation between measured and simulated values illustrates the simulation ability of this model coupled photosynthesis and transpiration.

4.4. Sensitivity analysis of the model

Sensitivity analyses were performed to see the response of the model under variable climatic environmental conditions. Frequently a model can perform well under small variation ranges of driving variables, but

may fail under large variation of these variables or extreme climatic conditions. There are large differences in the climatic and soil conditions in the different wheat growing regions in China. For example, the Tibet plateau has higher solar radiation and lower CO_2 partial pressure and lower air temperature than the North China Plain in the growing season of winter wheat. But in the Loess plateau, water deficit is the major factor limiting crop production (Li et al., 2001). Therefore, it is important to investigate the behavior of the model under various driving factors (temperature, light intensity, soil moisture and ambient CO_2 concentration).

Fig. 13 shows the response of latent heat flux (λE), canopy conductance (g_{sc}) and canopy net photosynthesis rate (A_{nc}) of winter wheat to the change in air temperature (0–45 °C) at five irradiance levels. Air temperature affects canopy photosynthesis and stomatal conductance by two ways, one is on the intrinsic speed of biochemical process of photosynthesis, and the other is on vapor pressure deficit (D_a). Clearly, an optimum temperature exists in the temperature response curves of λE, g_{sc} and A_{nc}. When air temperature is low, canopy photosynthesis is small due to the limitation by low temperature even at high light intensity. A_{nc}, g_{sc} and λE increase with increasing air temperature before the optimum temperature. When air temperature is larger than the optimum for g_{sc}, canopy conductance begins to decline. This is because an increase in air temperature will cause an exponential increase in D_a and the negative effect of D_a on stomatal conductance is larger than the positive effect of leaf temperature on stomatal conductance, and accordingly A_{nc} declines with

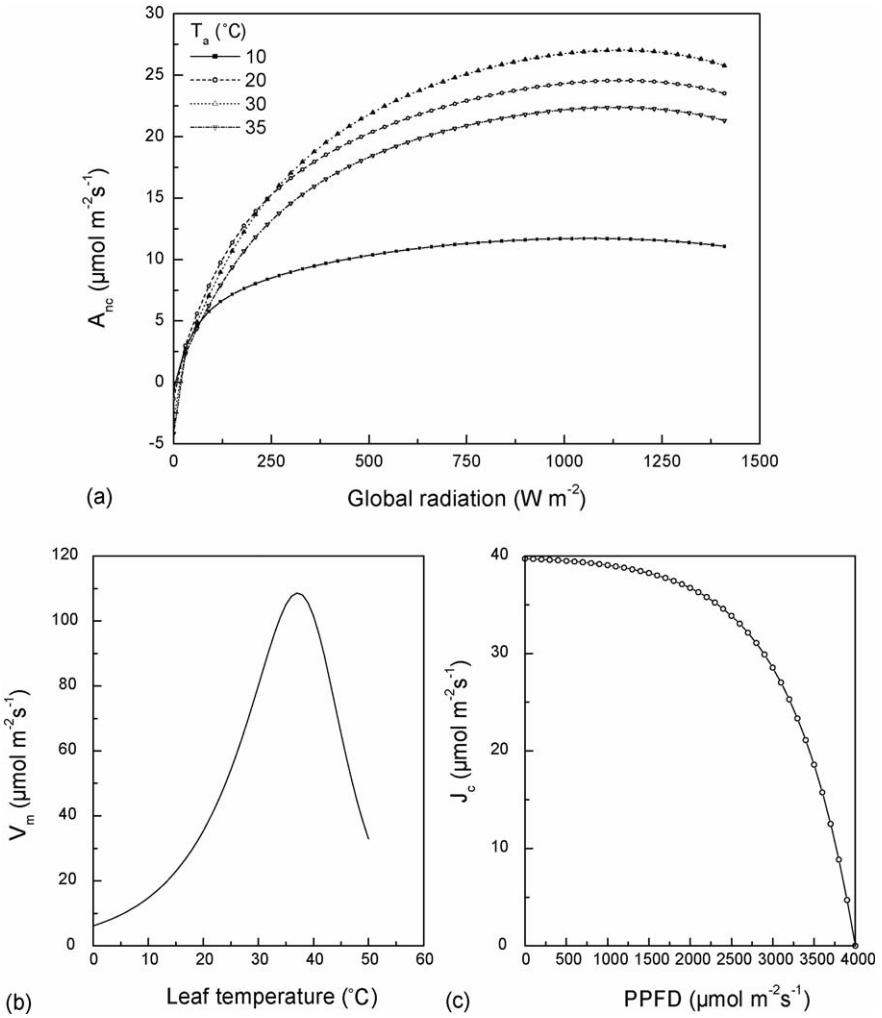

Fig. 14. The response of canopy net photosynthetic rate to the change in solar radiation at three temperature levels at relative humidity, 60% and wind speed, 2 m s^{-1}.

decreasing canopy conductance. There are two physiological responses of transpiration to the variation in D_a. An increase in canopy resistance will reduce transpiration. On the other hand, increasing D_a tends to increase water vapor flux from canopy to the atmosphere. When the negative effect of decreasing g_{sc} on transpiration is stronger than the positive effect of increasing D_a, transpiration and λE decrease. Therefore, the optimum temperature of g_{sc} is lower than A_{nc} and λE. Moreover, there is a shift of the optimum of A_{nc} and g_{sc} toward higher temperatures with increasing solar radiation. For example, the optimum temperature is 22 °C at $R_g = 200$ W m^{-2} and it increased to 28 °C at $R_g = 400$ W m^{-2}. When solar radiation is very high and rises further, there is a little change in the optimum temperature. All these responses of the model under variations rages of air temperature (0–45 °C) and solar radiation accord with the results of many experiments and models (Jarvis, 1980; Nikolov et al., 1995; Cannell and Thornley, 1998).

The response of canopy net photosynthesis to the change in solar radiation at four temperatures is presented in Fig. 14a. Solar radiation provides the energy for photosynthesis and affects the leaf energy balance which determines leaf temperature. Canopy photosynthesis responds the irradiance in a Michaelis–Menten curve before the light saturation point. The maximum photosynthesis is determined by the maximum catalytic capacity of Rubisco (V_m) which depends on leaf temperature (Fig. 14b). Then canopy photosynthesis declines when light intensity exceeds the light saturation point, this is because high light intensity greatly inhibits photosynthesis, and this phenomenon can be observed in the Tibet plateau (Yu et al., 2002). In our model, we modeled this phenomenon by the decrease of maximum photosynthetic rate with increasing light intensity (Fig. 14c).

The modeled response of canopy conductance (g_{sc}), CO_2 flux (F_c) and latent heat flux (λE) to the change in soil water content is shown in Fig. 15. When soil water limiting, the midday depression of g_{sc} is aggravated with an evident parallel depression of F_c. An increase in canopy resistance and soil resistance lead to a diminishment of λE. Canopy conductance increases with increasing soil water content, and it is not any longer a limiting factor of g_{sc} when soil is well-watered.

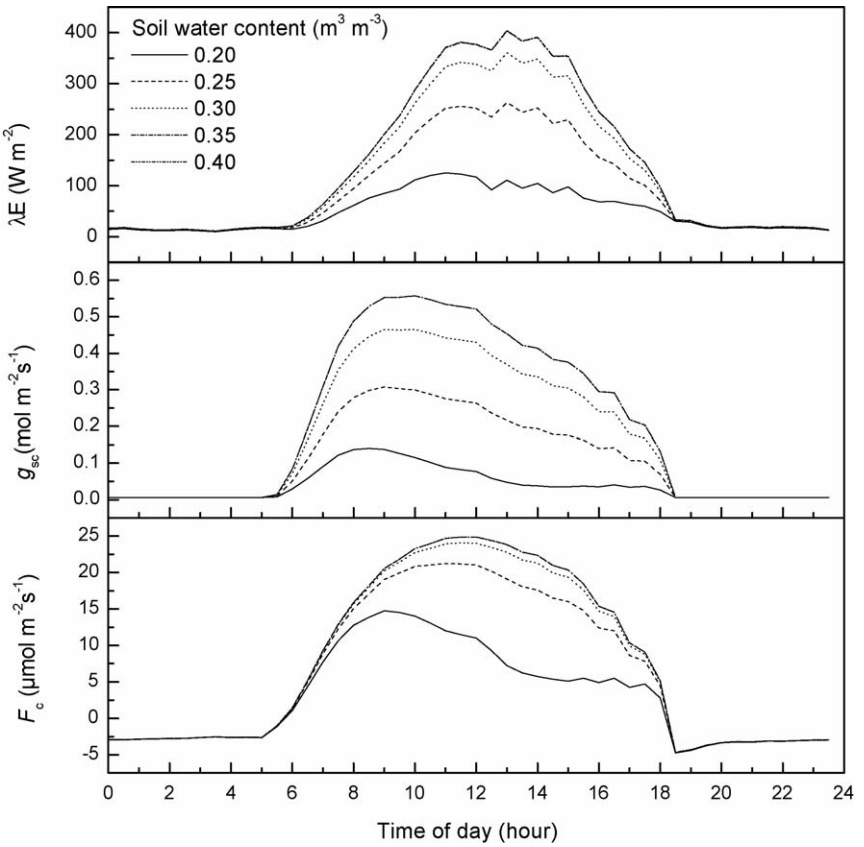

Fig. 15. The response of canopy conductance (g_{sc}), CO_2 flux (F_c) and latent heat flux (λE) to the change in soil water content.

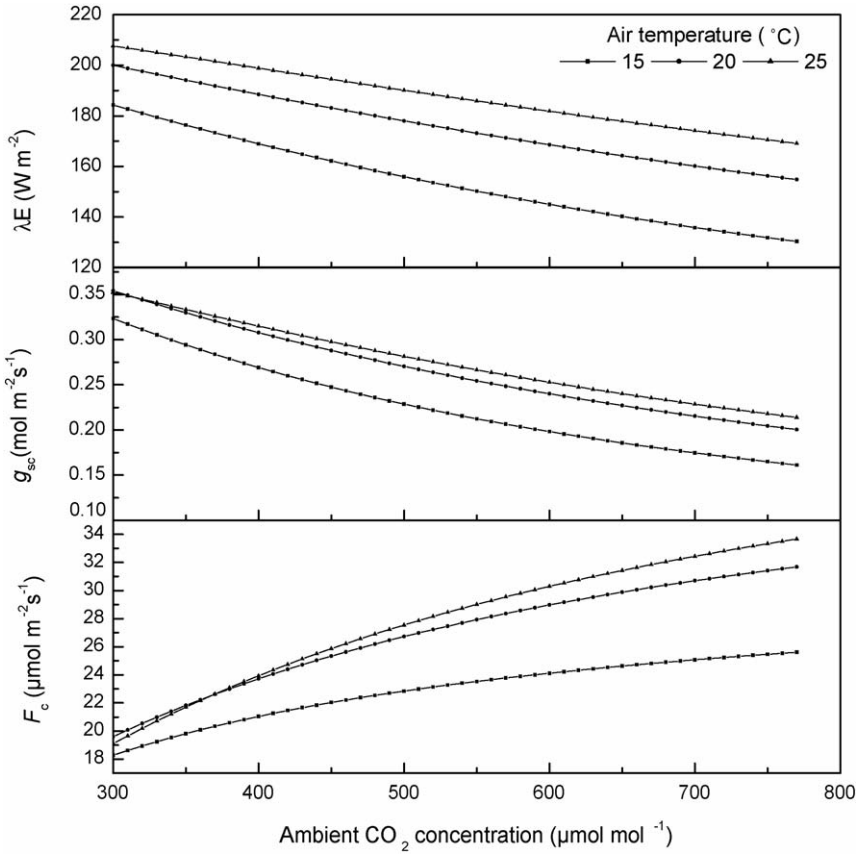

Fig. 16. The responses of canopy conductance (g_{sc}), CO_2 flux (F_c) and latent heat flux (λE) to the change in ambient CO_2 concentration (C_a) at three temperature levels at wind speed, 2 m s^{-1}; vapor water deficit, 1 kPa; global radiation, 600 W m^{-2}.

Modeled responses of variations of canopy conductance (g_{sc}), CO_2 flux (F_c), latent heat flux (λE) to the change in ambient CO_2 concentration (C_a) at three temperatures is presented in Fig. 16. An increase in ambient CO_2 concentration results in a decrease in g_{sc} that may be caused by a nearly linear increase in CO_2 concentration over the leaf surface (C_s) and the intercellular CO_2 concentration (C_i). And canopy photosynthesis increases with increasing C_i according to the photosynthesis model. However, canopy resistance will increase due to decreasing g_{sc}, which results in a decrease in crop transpiration and latent heat flux. Thus, WUE may increase when C_a increases. These conclusions support of the results of many experiments reported earlier (Eamus, 1991; Reynold et al., 1992). And we can see from Fig. 14, the effect of increased ambient CO_2 concentration on photosynthesis is larger at higher temperature. The phenomenon was observed in CO_2 enrichment experiments (Idso and Idso, 1994) and was modeled in crop growth models (Nonhebel, 1996).

5. Conclusion

Measurements taken in the North China Plain showed that diurnal variation of CO_2, water and heat fluxes were determined by the interactive effect of environmental factors although solar radiation is the dominant factor. There is an evident midday depression of photosynthesis of winter wheat caused by stomatal closure due to excessive transpiration caused by high canopy temperature and water vapor deficit. The coupled photosynthesis and transpiration model developed here take into consideration the physiological and physical processes of CO_2, water and heat fluxes for the main agricultural region in China. Satisfactory agreement was obtained between simulated and measured fluxes of CO_2, net radiation, sensible and latent heat, which shows the strong simulating power of the model. Sensitivity analyzes indicated the model can reflect the response of CO_2, water and heat fluxes to changes in solar radiation, air temperature, soil moisture and ambient CO_2 concentration. The models presented here

provide a sound mechanism to study CO_2, water and heat exchange between the cropland and atmosphere and could be extrapolated to other climatic regions in China, such as the Losses plateau and the Tibet plateau. The model can be used to simulate CO_2, water and heat flux of wheat not only under present climatic conditions, but also under future climatic conditions.

Acknowledgements

This work is supported by Significant Item of Knowledge Innovation Project of the Chinese Academic of Science (KZCX1-SW-01-01A), the Ministry of Science and Technology of China (2002CB412501), and National Natural Science Foundation of China (No. 40328001). We wish to acknowledge the valuable comments and revision by Dr. Ray Leuning of the contents of this work.

Appendix A

A.1. The calculation of extinction coefficient and albedo

The values of extinction coefficients for direct visible radiation and direct infrared radiation in a canopy are (Goudriaan, 1977):

$$k_v(i) = 0.0353 + 0.94623 \times k_{hv} \times k_b(i) \quad \text{(A1.1)}$$

$$k_i(i) = 0.0353 + 0.94623 \times k_{hi} \times k_b(i) \quad \text{(A1.2)}$$

in which i is from 1 to 9, which denotes the inclination angles of 0–10°, …, 81–90°, respectively. k_b is the extinction coefficient for a canopy with black leaves. k_{hv} and k_{hi} are extinction coefficients for a canopy with horizontal leaves for visible radiation and infrared radiation. The coefficient for diffuse radiation is described by:

$$\exp(-k_d L) = \sum_{i=1}^{9} B_u(i) \exp(k_f(i) L) \quad \text{(A1.3)}$$

where k_d is the extinction coefficient for diffuse radiation in a canopy with black leaves and B_u is the normal distribution of diffuse radiation. Thus, extinction coefficients for diffuse visible radiation and diffuse infrared radiation of a canopy are:

$$k_{dv} = \frac{-\ln\left(\sum_{i=1}^{9} B_u(i) e^{k_v(i)L}\right)}{L} \quad \text{(A1.4)}$$

and

$$k_{di} = \frac{-\ln\left(\sum_{i=1}^{9} B_u(i) e^{k_i(i)L}\right)}{L} \quad \text{(A1.5)}$$

Because the scattering coefficient σ is close to 0 for the attenuation of long wave radiation, the attenuation of long wave radiation is:

$$\exp(-k_l L) = \sum_{i=1}^{9} B_u(i) \exp(k_b(i) L) \quad \text{(A1.6)}$$

The extinction coefficient for long wave radiation of a canopy is:

$$k_l = \frac{-\ln\left(\sum_{i=1}^{9} B_u(i) e^{k_b(i)L}\right)}{L} \quad \text{(A1.7)}$$

The albedo of a canopy with horizontal leaves for direct visible radiation and direct infrared radiation is defined by:

$$\rho_{fv} = 1 - e^{-2\rho_{hv}(1+(L\times k_{dv})/(1+k_{dv}))\times(k_b/(1+k_b))} \quad \text{(A1.8)}$$

and

$$\rho_{fi} = 1 - e^{-2\rho_{hi}(1+(L\times k_{di})/(1+k_{di}))\times(k_b/(1+k_b))} \quad \text{(A1.9)}$$

The albedo of canopy for direct visible radiation and direct infrared radiation is given by:

$$\rho_v(i) = -0.0111544 + 1.117 \times \rho_{fv}(i) \quad \text{(A1.10)}$$

$$\rho_i(i) = -0.0111544 + 1.117 \times \rho_{fi}(i) \quad \text{(A1.11)}$$

The albedo of canopy for diffuse visible radiation and diffuse infrared radiation is:

$$\rho_{dv} = \sum_{i=1}^{9} B_u(i) \rho_v(i) \quad \text{(A1.12)}$$

$$\rho_{di} = \sum_{i=1}^{9} B_u(i) \rho_i(i) \quad \text{(A1.13)}$$

A.2. Two-layer evapotranspiration model

Latent heat fluxes of canopy and soil are estimated by S–W model (Shuttleworth and Wallace, 1985). The difference in vapor pressure and temperature between the level of mean canopy air flow and reference height

are calculated by:

$$e_x - e_0 = \frac{-\lambda E r_a^a \gamma}{\rho c_p} \quad (A2.1)$$

$$T_x - T_0 = \frac{-H r_a^a}{\rho c_p} \quad (A2.2)$$

Vapor pressure deficit at the canopy source height (D_0) is:

$$D_0 = e_w(T_x) - [e_w(T_x) - e_w(T_0)] - e_0 \quad (A2.3)$$

The relation between D_0 and D_a is:

$$D_0 = D_a + \frac{[\Delta(R_n - G) - (\Delta + \gamma)\lambda E] r_a^a}{\rho c_p} \quad (A2.4)$$

The total latent flux above the canopy is described by:

$$\lambda E = C_c PM_c + C_s PM_s \quad (A2.5)$$

where PM_c and PM_s are terms similar to those of the Penman–Monteith equation and they have the form:

$$PM_c = \frac{\Delta(R_n - G) + [\rho C_p D - \Delta r_a^c (R_{ns} - G)]/(r_a^a + r_a^c)}{\Delta + \gamma(1 + (r_s^c/r_a^a + r_a^s))} \quad (A2.6)$$

and

$$PM_s = \frac{\Delta(R_n - G) + [\rho C_p D - \Delta r_a^s (R_n - R_{ns})]/(r_a^a + r_a^s)}{\Delta + \gamma(1 + (r_s^s/r_a^a + r_a^s))} \quad (A2.7)$$

C_c and C_s are defined as

$$C_c = \frac{1}{1 + (R_c R_a/(R_s(R_c + R_a)))} \quad (A2.8)$$

and

$$C_s = \frac{1}{1 + (R_s R_a/(R_c(R_s + R_a)))} \quad (A2.9)$$

where R_a, R_c and R_s are defined as:

$$R_a = (\Delta + \gamma) r_a^a \quad (A2.10)$$

$$R_c = (\Delta + \gamma) r_a^c + \gamma r_s^c \quad (A2.11)$$

$$R_s = (\Delta + \gamma) r_a^s + \gamma r_s^s \quad (A2.12)$$

D_0 is determined by the total latent heat fluxes

$$D_0 = D_a + \frac{[\Delta(R_n - G) - (\Delta + \gamma)\lambda E] r_a^a}{\rho c_p} \quad (A2.13)$$

Then soil evaporation and crop transpiration are given by:

$$\lambda E_c = \frac{\Delta(R_n - R_{ns}) + \rho C_p D_0 / r_a^c}{\Delta + \gamma(1 + (r_s^c/r_a^c))} \quad (A2.14)$$

$$\lambda E_s = \frac{\Delta(R_{ns} - G) + \rho C_p D_0 / r_a^s}{\Delta + \gamma(1 + (r_s^s/r_a^s))} \quad (A2.15)$$

A.3. Leaf photosynthesis model

Farquhar et al. (1980) and von Caemmerer and Farquhar (1981) developed a biochemical model of leaf photosynthesis for C_3 plants, in which the gross photosynthetic rate (A) was expressed as a function of intercellular partial pressure of CO_2 (P_i), the incident photosynthetic photon flux density (Q_p) and leaf temperature (T_l).

$$A \approx \min \left\{ \begin{matrix} J_E,\ f(Q_p, a, P_i, T_l) \\ J_C,\ f(V_m, P_i, T_l) \\ J_S,\ f(T_l, V_m) \end{matrix} \right\} \quad (A3.1)$$

in which J_E is the rate limited solely by the regeneration capacity of ribulose bisphosphate (RuBP), which is for the substrate enzyme Rubisco, J_C the assimilation rate limited by the activation and kinetic properties of the enzyme Rubisco alone and J_S is the capacity for the utilization of the products of photosynthesis (most likely as sucrose synthesis).

Because the transition from the limitation by one factor to the limitation by another appears to be gradual, to allow for some co-limitation between J_C, J_E and J_S, Collatz et al. (1991) solved the following quadratics for their smaller roots.

$$\beta_1 J_P^2 - J_P(J_E + J_C) + J_E J_C = 0 \quad (A3.2)$$

$$\beta_2 A^2 - A(J_P + J_S) + J_P J_S = 0 \quad (A3.3)$$

where A is the gross rate of CO_2 uptake, J_P an intermediate variable which represents the smaller one of J_C and J_E and β_1 and β_2 are convexity coefficients describing the transition between limitations, and are close to one. The Rubisco-limited rate of photosynthesis is defined as (Collatz et al., 1991):

$$J_C = \frac{V_m(P_i - \Gamma)}{P_i + K_c(1 + O/K_o)} \quad (A3.4)$$

where V_m is the maximum rate of carboxylation at an ambient oxygen concentration of 21%, P_i and O the partial pressures of the CO_2 and O_2 in the intercellular air space of the leaf, Γ the CO_2 compensation point and K_c and K_o are the Michaelis–Menten kinetic parameters

for CO_2 and O_2 which are calculated from (Nikolov et al., 1995):

$$K_c = PK_{c25} \exp\left[32.462 - \frac{80470}{RT_l}\right] \quad (A3.5)$$

$$K_o = PK_{o25} \exp\left[5.854 - \frac{14510}{RT_l}\right] \quad (A3.6)$$

where P is the atmospheric pressure and K_{c25} and K_{o25} are the corresponding parameter values at 25 °C. If considering the inhibition of light intensity on the photosynthesis, the decrease of maximum photosynthetic rate (J_C) with increasing light intensity (I) can be described as (Yu et al., 2002):

$$J_{c0} = J_c\left\{1 - \exp\left[f\left(\frac{I}{I_m} - 1\right)\right]\right\} \quad (A3.7)$$

in which f is a parameter characterizing the relative rate of decrease and I_m is the maximal light intensity under which photosynthetic rate achieves 0.

RuBP regeneration is controlled by the rate of electron transport/photophosphorylation which is given by (Collatz et al., 1991):

$$J_E = \alpha_0 Q_a \frac{P_i - \Gamma}{P_i + 2\Gamma} \quad (A3.8)$$

where α_0 is the intrinsic quantum efficiency for CO_2 uptake and Q_a is the leaf absorbed photosynthetically active radiation.

The gross assimilation rate limited by the triose phosphate utilization is defined as (Collatz et al., 1991):

$$J_s = \frac{V_m}{2} \quad (A3.9)$$

V_m depends on leaf temperature (T_l) (Collatz et al., 1991):

$$V_m = V_m^0\left\{1 + \exp\left[\frac{-a_1 + a_2 T_l}{RT_l}\right]\right\}^{-1} \quad (A3.10)$$

where

$$V_m^0 = V_{m25} Q_{10}^{(T_a - 25)/10} \quad (A3.11)$$

in which a_1 and a_2 are the parameters and V_m^0 is an intermediate variable. V_{m25} is V_m^0 at 25 °C. Dark respiration (R_d) is proportional to V_m (Collatz et al., 1991):

$$R_d = rV_m \quad (A3.12)$$

in which r is a proportionality constant. Then leaf net photosynthetic rate (A_n) can be obtained by the expression:

$$A_n = A - R_d \quad (A3.13)$$

A.4. Stomatal conductance model

Ball et al. (1987) proposed a semi-empirical stomatal model in which stomatal conductance was expressed as a function of relative humidity and CO_2 concentration (C_s) over leaf surface and net photosynthetic rate (A_n) under conditions of ample water supply. The relation was revised by replacing relative humidity over leaf surface with water vapor saturation deficit over leaf surface (D_s) (Leuning, 1995; Wang and Leuning, 1998) with the following equation:

$$g_s = m\frac{A_n}{(C_s - \Gamma)(1 + D_s/D_0)} + g_0 \quad (A4.1)$$

where Γ is the CO_2 compensation point, D_0 a parameter reflecting the response of stomata to atmospheric vapor saturation deficit, m an empirical parameter and g_0 is the intercept. Here we introduce a limiting factor of soil moisture on stomatal conductance $f(\theta)$ (Gollan et al., 1986; Wang and Leuning, 1998) and (A4.1) can be written newly,

$$g_s = m\frac{A_n}{(C_s - \Gamma)(1 + D_s/D_0)} f(\theta) + g_0 \quad (A4.2)$$

in which $f(\theta) = m_1((\theta - \theta_w)/(\theta_f - \theta_w))$, θ is the average soil water content between 0 and 20 cm depth, θ_w and θ_f the soil water content at the wilting point and at the field capacity, m_1 the field capacity and m_1 is a empirical constant.

A.5. Gaseous diffusion model

Aphalo and Jarvis (1993) derived an expression of D_s as a function of D_a, under the assumption that $T_l = T_a$,

$$D_s = D_a\left(1 - \frac{g_{tw}}{g_{bw}}\right) \quad (A5.1)$$

where D_a is the water vapor saturation deficit from intercellular and ambient air and g_{tw} and g_{bw} are the total conductance and boundary layer conductance to water vapor, respectively.

The relation between g_{sw} with g_{sc} and overall stomatal conductance to CO_2 (g_{tc}) can be expressed as follows:

$$g_{sw} = 1.6 g_{sc} \quad (A5.2)$$

$$g_{tw} = \frac{1}{((1/g_{sw}) + (1/g_{bw}))} \quad (A5.3)$$

$$g_{tc} = \frac{1}{((1.6/g_{sw}) + (1.37/g_{bw}))} \quad (A5.4)$$

According to flux–gradient relation, there are the following relations:

$$C_s = C_a - \frac{P_n}{g_{bc}} \quad \text{(A5.5)}$$

$$C_i = C_a - \frac{P_n}{g_{tc}} \quad \text{(A5.6)}$$

where g_{bc} is boundary layer conductance to CO_2.

Appendix B

Table B.1 The variables and parameters in the model

Symbol	Variables and parameters	Unit
A	Leaf gross photosynthetic rate	μmol m^{-2} s^{-1}
A_n	Leaf net photosynthetic rate	μmol m^{-2} s^{-1}
A_{nc}	Canopy net photosynthetic rate	μmol m^{-2} s^{-1}
C_a	Ambient CO_2 concentration	μmol mol^{-1}
C_i	Intercellular CO_2 concentration	μmol mol^{-1}
C_s	CO_2 concentration over leaf area	μmol mol^{-1}
C_p	The constant pressure of specific heat	J kg^{-1} K^{-1}
d	Zero plane displacement	m
D	Soil layer thickness	m
D_a	Air vapor saturation deficit	h Pa
D_0	Vapor saturation deficit at canopy source height	h Pa
D_s	Vapor saturation deficit over leaf surface	h Pa
E_c	Crop transpiration	mm s^{-1}
F_c	CO_2 flux above the canopy	μmol m^{-2} s^{-1}
F_n	Surface effective radiation	W m^{-2}
g_{bc}	Boundary layer conductance to CO_2	m s^{-1}
g_{bw}	Boundary layer conductance to water vapor	m s^{-1}
g_s	Leaf stomatal conductance to CO_2	m s^{-1}
g_{sc}	Canopy conductance to CO_2	m s^{-1}
g_{sw}	Canopy conductance to H_2O	m s^{-1}
g_{tc}	Total conductance to CO_2	m s^{-1}
g_{tw}	Total conductance to water vapor	m s^{-1}
G	Soil heat flux	W m^{-2}
h	Crop height	m
H	Sensible heat flux above the canopy	W m^{-2}
H_c	Sensible heat flux of canopy	W m^{-2}
H_s	Sensible heat flux of soil	W m^{-2}
I	Light intensity	W m^{-2}
I_0	Light density at the top of the canopy	W m^{-2}
I_1	Irrigation amount	mm s^{-1}
I_m	Maximal light density	μmol m^{-2} s^{-1}
J_C	CO_2-limited and RuBP-saturated rate of photosynthesis	μmol m^{-2} s^{-1}
J_E	RuBP-limited rate of photosynthesis	μmol m^{-2} s^{-1}
J_s	Sink capacity	μmol m^{-2} s^{-1}
k	von Karman's constant	–
k_b	Extinction coefficient of canop with black leaves for direct radiation	–
k_d	Extinction coefficient of canopy with black leaves for diffuse radiation	–
k_{di}	Extinction coefficient of canopy for diffuse infrared radiation	–
k_{dv}	Extinction coefficient of canopy for diffuse visible radiation	–
k_f	Extinction coefficient of canopy for direct radiation	–
k_l	Extinction coefficient of canopy for long wave radiation	–
k_{bv}	Extinction coefficient of canopy with horizontal leaves for visible radiation	–
k_{hi}	Extinction coefficient of canopy with horizontal leaves for infrared radiation	–
K_c	Michaelis–Menten kinetic parameter for CO_2	Pa
K_o	Michaelis–Menten kinetic parameter for O_2	Pa
$K(z)$	Soil heat conductivity	°C m^{-1}
L	Leaf area index	–
L_r	Root length	m
n	Layer number of soil	–
O	Partial pressure of O_2	Pa
P	Atmospheric pressure	Pa
P_i	Partial pressure of CO_2	Pa
P_1	Precipitation	mm s^{-1}
Q	Water flux at an interface between two adjacent compartments	s m^{-1}
r_a^a	Aerodynamic resistance between the canopy source height and reference height	s m^{-1}
r_a^c	Boundary resistance of canopy	s m^{-1}
r_a^s	Aerodynamic resistance between the substrate and canopy source height	s m^{-1}
r_s^c	Canopy resistance	s m^{-1}
r_s^s	Soil resistance	s m^{-1}
R	Universal gas constant	J mol^{-1} K^{-1}
R_d	Dark respiration	μmol m^{-2} s^{-1}
R_g	The global radiation	W m^{-2}
R_{lc}	Long wave radiation of the canopy	W m^{-2}
R_{ls}	Long wave radiation of the soil	W m^{-2}
R_n	Net radiation above the canopy	W m^{-2}
R_{nc}	Net radiation absorbed by the canopy	W m^{-2}
R_{ns}	Net radiation absorbed by the soil	W m^{-2}
R_s	Soil respiration	μmol m^{-2} s^{-1}
S	Root uptake rate	mm s^{-1}
S_{di}	Direct infrared radiation	W m^{-2}
S_{dv}	Direct visible radiation	W m^{-2}
S_{si}	Diffuse infrared radiation	W m^{-2}
S_{sv}	Diffuse visible radiation	W m^{-2}
t	Time	s
T_a	Air temperature at reference height	°C
T_c	Canopy temperature	°C
T_g	Ground temperature	°C

Appendix B (*Continued*)

T_l	Leaf temperature	°C
T_r	Transpiration rate	m s^{-1}
T_s	Soil temperature	°C
u_*	Friction velocity	m s^{-1}
u_h	Wind speed at canopy height	m s^{-1}
u_r	Wind speed at reference height	m s^{-1}
V_m	Maximum rate of carboxylation	μmol m^{-2} s^{-1}
z_b	Roughness length of bare soil surface	m
z_0	Roughness length of canopy	m
α_0	The intrinsic quantum efficiency for CO_2 uptake	–
β_1	Convexity coefficient	–
β_2	Convexity coefficient	–
γ	The psychometric constant	Pa $°C^{-1}$
θ	Soil water content	m^3 m^{-3}
θ_s	Saturated soil water content at 0-5 mm	m^3 m^{-3}
θ_f	Soil water content at the wilting point	m^3 m^{-3}
θ_w	Soil water content at the field capacity	m^3 m^{-3}
λE	Latent heat flux above the canopy	W m^{-2}
λE_c	Latent heat flux of canopy	W m^{-2}
λE_s	Latent heat flux of soil	W m^{-2}
ψ	Soil water potential	m
ρ	Air density	kg m^{-3}
ρ_a	Albedo of canopy and soil to solar radiation	–
ρ_{dv}	Albedo of canopy for diffuse visible radiation	–
ρ_{di}	The albedo of canopy for diffuse infrared radiation	–
ρ_{fv}	Albedo of canopy with horizontal leaves for visible radiation	–
ρ_{fi}	Albedo of canopy with horizontal leaves for infrared radiation	–
ρ_v	Albedo of canopy for direct visible radiation	–
ρ_i	Albedo of canopy for direct infrared radiation	–
Δ	Slope of saturation vapor press versus temperature curve	Pa $°C^{-1}$
Γ	CO_2 compensation point	Pa
σ	The Stefan–Boltzmann constant	W m^{-2} K^{-4}
σ_α	Momentum partition coefficient	–

References

Amthor, J.S., 1994. Scaling CO_2–photosynthesis relationships from the leaf to the canopy. Photosynth. Res. 39, 321–350.

Anadranistakis, M., Kerkides, P., Liakatas, A., Alexandris, S., Poulovassilis, A., 1999. How significant is the usual assumption of neutral stability in evapotranspiration estimating models. Meteorology 6, 155–158.

Anadranistakis, M., Liakatas, A., Kerkides, P., Rizos, S., Gavanosis, J., Poulovassilis, A., 2000. Crop water requirements model tested for crops grown in Greece. Agric. Water Manage. 45, 297–316.

Aphalo, P.J., Jarvis, P.G., 1993. The boundary layer and the apparent responses of stomatal conductance to wind speed and to the mole fraction of CO_2 and water vapour in the air. Plant Cell Environ. 16, 771–783.

Baldocchi, D.D., 1992. A lagrangian random walk model for simulating water vapor, CO_2 and sensible heat flux densities and scalar profiles over and within a soybean canopy. Boundary-layer Meteorol. 61, 113–144.

Baldocchi, D.D., Harley, P.C., 1995. Scaling carbon dioxide and water vapor exchange from leaf to canopy in a deciduous forest. II. Model testing and an application. Plant Cell Environ. 18, 1157–1173.

Ball, J.T., 1987. Calculations related to gas exchange. In: Zeiger, E., Farquhar, G.D., Cowan, I.R. (Eds.), Stomatal Function. Stanford University Press, Stanford, pp. 445–476.

Ball, J.T., Woodrow, I.E., Berry, J.A., 1987. A model predicting stomatal conductance and its contribution to the control of photosynthesis under different environmental conditions. In: Biggens, J. (Ed.), Progress in Photosynthesis Research, vol. IV. Martinus Nijhoff, Dordrecht, pp. 221–224.

Brutsaert, W.H., 1988. Evaporation into the Atmosphere. Reidel, Dordrecht.

Brutsaert, W., Stricker, H., 1979. An advection–aridity approach to estimate actual regional evapotranspiration. Water Resour. Res. 15, 443–450.

Cannell, M.G.R., Thornley, J.H.M., 1998. Temperature and CO_2 responses of leaf and canopy photosynthesis: a clarification use the non-rectangular hyperbola model of photosynthesis. Ann. Botany 82, 883–892.

Chen, J., 1984. Uncoupled multi-layer model for the transfer of sensible and latent heat flux densities from vegetation. Boundary-layer Meteorol. 28, 213–225.

Chen, J.M., Liu, J., Cihlar, J., Goulden, M.L., 1999. Daily canopy photosynthesis model through temporal and spatial scaling for remote sensing applications. Ecol. Model. 124, 99–119.

Choudhury, B.J., Monteith, J.L., 1988. A four-layer model for the heat budget of homogenous land surfaces. Q. J. R. Meteorol. Soc. 114, 373–398.

Collatz, G.J., Ball, J.T., Grivet, C., Berry, J.A., 1991. Physiological and environmental regulation of stomatal conductance, photosynthesis and transpiration: a model that includes a laminar boundary layer. Agric. For. Meteorol. 54, 107–136.

Domingo, F., Villagarcia, L., Brenner, A.J., Puigedefabregas, J., 1999. Evapotranspiration model for semi-arid shrub lands tested against data from SE Spain. Agric. For. Meteorol. 95, 67–84.

Eamus, D., 1991. The interaction of rising CO_2 and temperature with water use efficiency. Plant Cell. Environ. 14, 543–582.

Farquhar, G.D., von, C.S., Berry, J.A., 1980. A biochemical model of photosynthetic CO_2 assimilation in leaves of C_3 species. Planta 149, 78–90.

Farquhar, G.D., 1989. Models of integrated photosynthesis of cells and leaves. Philos. Trans. R. Soc. Lond. B 323, 357–367.

Feddes, R., Zaradny, H., 1978. Model for simulating soil water content considering evapotranspiration-comments. J. Hydrol. 37, 393–397.

Garratt, J.R., 1978. Transfer characteristics for a heterogeneous surface of large aerodynamic roughness. Q. J. R. Meteorol. Soc. 104, 491–502.

Gollan, T., Passioura, J.B., Munns, R., 1986. Soil water status affects the stomatal conductance of fully turgid wheat and sunflower leaves. Aust. J. Plant Physiol. 13, 459–464.

Goudriaan, J., 1977. Crop Micrometeorology: A Simulation Study. Center for Agricultural Publishing and Documentation, Wageningen, The Netherlands.

Hirasawa, T., Iida, Y., Ishihara, K., 1989. Dominant factors in reduction of photosynthetic rate affected by air humidity and leaf water potential in rice plants. Jpn. J. Crop Sci. 58, 383–389.

Hirasawa, T., Hsiao, T.C., 1999. Some characteristics of reduced leaf photosynthesis at midday in maize growing in the field. Field Crops Res. 62, 53–62.

Idso, K.E., Idso, S.B., 1994. Plant responses to atmospheric CO_2 enrichment in the in the face of environmental constraints: a review of the past 10 years research. Agric. For. Meteorol. 69, 154–203.

Ishihara, K., Saito, K., 1987. Diurnal course of photosynthesis, transpiration, and diffusive conductance in the single leaf of the rice plants grown in the paddy field under submerged condition. Jpn. J. Crop Sci. 56, 8–17.

Jarvis, P.G., 1976. The interpretation of the variations in leaf water potential and stomatal conductance found in canopies in the field. Philos. Trans. R. Soc. Lond. Ser. B 273, 593–610.

Jarvis, P.G., 1980. Stomatal response to water stress in conifers. In: Turner, N.C., Kramer, P.J. (Eds.), Adaptation of Plants to Water and High Temperature Stress. Wiley/Interscience, New York, pp. 105–122.

Jensen, M.E., Burman, R.D., Allen, R.G., 1990. Evapotranspiration and Irrigation Water Requirements. Irrigation and Drainage Division ASCE. ASCE Manuals and Reports on Engineering Practice No. 70, 332 pp.

Katul, G.G., Parlange, M.B., 1992. A Penman–Brutsaert model for wet surface evaporation. Water Resour. Res. 28, 121–126.

Konzelmann, T., Calanca, P., Mü1ler, G., Menzel, L., Lang, H., 1997. Energy balance and evapotranspiration in a high mountain area during summer. J. Appl. Meteorol. 36, 966–973.

Kull, O., Jarvis, P., 1995. The role of nitrogen in a simple scheme to scale up photosynthesis from leaf to canopy. Plant Cell Environ. 18, 1174–1182.

Kustas, W.P., 1990. Estimations of evapotranspiration with one and two-dimension model of heat transfer over partial canopy cover. J. Appl. Meterorol. 29, 704–715.

Larson, E.M., Hesketh, J.D., Woolley, J.T., Peters, D.B., 1981. Seasonal variations in apparent photosynthesis among plant stands of different soybean cultivars. Photosynth. Res. 2, 3–20.

Leyton, L., 1975. Fluid Behaviour in Biological Systems. Oxford, Clarendon Press, pp. 167–175.

Leuning, R., 1995. A critical appraisal of a combined stomatal–photosynthesis model for C_3 plants. Plant Cell Environ. 18, 339–355.

Leuning, R., Kelliher, F.M., De Pury, D.G., Schulze, E.D., 1995. Leaf nitrogen, photosynthesis, conductance and transpiration: scaling from leaves to canopies. Plant Cell Environ. 18, 1183–1200.

Leuning, R., Tuzet, A., Perrier, A., 2004. Stomata as part of the soil–plant–atmosphere continuum. In: Mencuccini, M., Grace, J., Moncrieff, J., McNaughton, K.G. (Eds.), Forests at the Land–Atmosphere Interface. pp. 9–28.

Li, F.M., Yan, X., Li, F.R., 2001. Effects of different water supply regimes on water use and yield performance of spring wheat in a simulated semi-arid environment. Agric. Water Manage. 47, 25–35.

Lin, J.D., Sun, S.F., 1983. Moisture and heat flow in soil and theirs effects on bare soil evaporation. Trans. Water Conservancy 7, 1–7 (in Chinese).

Luo, Y., Ouyang, Z., Yu, Q., Tang, D.Y., 2001. An integrated model for water, sensible heat and CO_2 fluxes and photosynthesis in SPAC system. II. Verification. Acta Hydrol. Sin. 26, 58–63.

Mehrez, B.M., Taconet, O., Vidal-Madjar, D., Valencogne, C., 1992. Estimation of stomatal resistance and canopy evaporation during the Hapex–Mobilhy experiment. Agric. For. Meteorol. 58, 285–313.

Monteith, J.L., 1965. Evaporation and environment. Symp. Soc. Exp. Biol. 19, 205–234.

Nikolov, N.T., Massman, W.J., Schoettle, A.W., 1995. Coupling biochemical and biophysical processes at the leaf level: an equilibrium photosynthesis model for leaves of C_3 plants. Ecol. Model. 80, 205–235.

Noilhan, J., Planton, S., 1989. A simple parameterization of land surface processes for meteorological models. Mon. Wea. Rev. 117, 536–549.

Nonhebel, S., 1996. Effects of temperature rise and increase in CO_2 concentration on simulated wheat yield in Europe. Climatic Change 34, 73–90.

Norman, J.M., 1980. Interfacing leaf and canopy light interception models. In: Hesketh, J.D., Jones, J.W. (Eds.), Predicting Photosynthesis for Ecosystem Models, vol. II, CRC Press, Boca Raton, FL, pp. 49–67. Stochastic modeling of radiation regime in discontinuous vegetation canopies. Remote Sens. Environ. 74, 125–144.

Norman, J., 1985. Modeling the complete crop canopy. In: Baarfield, B., Gerber, J. (Eds.), Modification of the Aerial Environment of Crops. Am. Soc. Agric. Eng. Monograph No. 2, ASAE, St. Joseph, MI, pp. 249–277.

Norman, J.M., 1993. Scaling processes between leaf and canopy levels. In: Ehleringer, J.R., Field, C.B. (Eds.), Scaling Physiological Processes: Leaf to Globe. Academic Press, San Diego, CA, pp. 41–76.

Parlange, M.B., Katul, G.G., 1992. An advection–aridity evaporation model. Water Resour. Res. 28, 127–132.

Penman, H.L., 1948. Natural evaporation from open water, bare soil and grass. Proc. R. Soc. 193, 120–145.

Pettigrew, W.T., Hesketh, J.D., Peters, D.B., Woolley, J.T., 1990. A vapor pressure deficit on crop canopy photosynthesis. Photosynth. Res. 24, 27–34.

Reynold, J.F., Chen, J.L., Harley, P.C., 1992. Modeling the effects of elevated CO_2 on plants: extrapolating leaf response to a canopy. Agric. For. Meterorol. 61, 69–94.

Sellers, P.J., Berry, J.A., Collatz, G.J., Field, C.B., Hall, F.G., 1992. Canopy reflectance, photosynthesis. Remote Sens. Environ. 42, 187–216.

Shuttleworth, W.J., Wallace, J.S., 1985. Evaporation from sparse crops—an energy combination theory. Q. J. R. Meteorol. Soc. 111, 839–855.

Shaw, R.H., Pereira, A.R., 1981. Aerodynmaic roughness of vegetated surfaces. The effect of canopy structure and density. 15th Conference of Agriculture and Forest Meteorology and 5th Conference on Biometeorology, Anaheim, CA, Am. Meteorol. Soc., 11–13 April 1981.

Tanaka, K., Kosugi, Y., Ohte, N., Kobashi, S., Nakamura, A., 1998. Model of CO_2 flux between a plant community and the atmosphere, and simulation of CO_2 flux over a planted forest. Jpn. J. Ecol. 48, 265–286 (in Japanese, with English abstract).

Tazaki, T., Ishihara, K., Ushijima, T., 1980. Influence of water stress on the photosynthesis and productivity of plants in humid area. In: Turner, N.C., Kramer, P.J. (Eds.), Adaptation of Plants to

Water and High Temperature Stress. Wiley, New York, pp. 309–321.

Tuzet, A., Perrier, A., Leuning, R., 2003. A coupled model of stomatal conductance, photosynthesis and transpiration. Plant Cell Environ. 26, 1097–1116.

Van Bavel, C.H.M., Hillel, D.I., 1976. Calculating potential and actual evaporation from a bare soil surface by simulation of concurrent flow of water and heat. Agric. Meteorol. 17, 453–476.

von Caemmerer, S., Farquhar, G.D., 1981. Some relationships between the biochemistry of photosynthesis and the gas exchange of leaves. Planta 153, 376–387.

Wang, Y.P., Leuning, R., 1998. A two-leaf model for canopy conductance, photosynthesis and partitioning of available energy. I. Model description and comparison with a multi-layered model. Agric. For. Meteorol. 91, 89–111.

Wu, J., Liu, Y., Jelinski, D.E., 2000. Effects of leaf area profiles and canopy stratification on simulated energy fluxes: the problem of vertical spatial scale. Ecol. Model. 134, 283–297.

Yu, Q., Goudriaan, J., Wang, T.D., 2001. Modeling diurnal courses of photosynthesis and transpiration of leaves on the bases of stomatal and non-stomatal responses, including photoinhibition. Photosynthetica 39, 43–51.

Yu, Q., Liu, Y.F., Liu, J.D., Wang, T.D., 2002. Simulation of leaf photosynthesis of winter wheat on Tibetan plateau and in North China Plain. Ecol. Model. 155, 205–216.